Pathology - Research and Practice 248 (2023) 154614

Contents lists available at ScienceDirect

Pathology - Research and Practice

journal homepage: www.elsevier.com/locate/prp

Single cell RNA-seq analysis with a systems biology approach to recognize important differentially expressed genes in pancreatic ductal adenocarcinoma compared to adjacent non-cancerous samples by targeting pancreatic endothelial cells

Elena Jamali [a,1], Arash Safarzadeh [b,1], Bashdar Mahmud Hussen [c], Thomas Liehr [d,*], Soudeh Ghafouri-Fard [e,*], Mohammad Taheri [d,f,**]

[a] Department of Pathology, Loghman Hakim Hospital, Shahid Beheshti University of Medical Sciences, Tehran, Iran
[b] Phytochemistry Research Center, Shahid Beheshti University of Medical Sciences, Tehran, Iran
[c] Department of Clinical Analysis, College of Pharmacy, Hawler Medical University, Kurdistan Region, Iraq
[d] Institute of Human Genetics, Jena University Hospital, Jena, Germany
[e] Department of Medical Genetics, School of Medicine, Shahid Beheshti University of Medical Sciences, Tehran, Iran
[f] Urology and Nephrology Research Center, Shahid Beheshti University of Medical Sciences, Tehran, Iran

ARTICLE INFO

Keywords:
Pancreatic ductal adenocarcinoma (PDAC)
ScRNA-seq
LncRNA
MiRNA
Endothelial cell

ABSTRACT

Pancreatic ductal adenocarcinoma (PDAC) is a cancer that is usually diagnosed at late stages. This highly aggressive tumor is resistant to most therapeutic approaches, necessitating identification of differentially expressed genes to design new therapies. Herein, we have analyzed single cell RNA-seq data with a systems biology approach to identify important differentially expressed genes in PDAC samples compared to adjacent non-cancerous samples. Our approach revealed 1462 DEmRNAs, including 1389 downregulated DEmRNAs (like PRSS1 and CLPS) and 73 upregulated DEmRNAs (like HSPA1A and SOCS3), 27 DElncRNAs, including 26 downregulated DElncRNAs (like LINC00472 and SNHG7) and 1 upregulated DElncRNA (SNHG5). We also listed a number of dysregulated signaling pathways, abnormally expressed genes and aberrant cellular functions in PDAC which can be used as possible biomarkers and therapeutic targets in this type of cancer.

1. Introduction

Pancreatic ductal adenocarcinoma (PDAC) is a cancer that is usually diagnosed at late stages, thus there is no chance of curative tumor resection [18]. This highly aggressive tumor is resistant to most therapeutic approaches, therefore there is a need for identification of differentially expressed genes in this type of cancer to design new therapies. Microarray-based approaches have been used in PDAC samples to find new tumor biomarkers and potential therapeutic targets [12]. One of the most prevalent and widespread cell types in the mammalian embryo are endothelial cells. These cells develop near and frequently as a component of various organs, including the kidneys, lungs, liver, and pancreas [26]. Islet endothelial cells interact physically and functionally with beta cells, and they also stimulate insulin gene transcription throughout islet progression, influence adult beta cell activity, encourage beta cell growth, and create a variety of growth factors. These cells also deliver oxygen and nutrients to endocrine cells [41]. More recently, the arrival of next-generation sequencing technologies, has revolutionized this field, since RNA sequencing (RNA-seq) is superior to microarray techniques in terms of high sensitivity and its capacity to identify splicing isoforms and somatic mutations [35]. Transcriptome analyses of PDAC cells have been successfully accomplished in PDAC cell lines [16], tumor cells detected in the circulation [40] and paired tumor samples and adjacent non-tumoral samples [24]. The latter approach has revealed several differentially expressed genes and abnormally activated pathways [24]. Moreover, next-generation whole-exome sequencing has been used to uncover driver mutations and abnormally activated signaling pathways in this type of cancer [34]. However, the application

* Corresponding authors.
** Corresponding author at: Institute of Human Genetics, Jena University Hospital, Jena, Germany.
E-mail addresses: Thomas.liehr@uni.med-jena.de (T. Liehr), s.ghafourifard@sbmu.ac.ir (S. Ghafouri-Fard), mohammad.taheri@uni-jena.de (M. Taheri).
[1] Contributed equally to this work

https://doi.org/10.1016/j.prp.2023.154614
Received 3 May 2023; Received in revised form 3 June 2023; Accepted 10 June 2023
Available online 13 June 2023

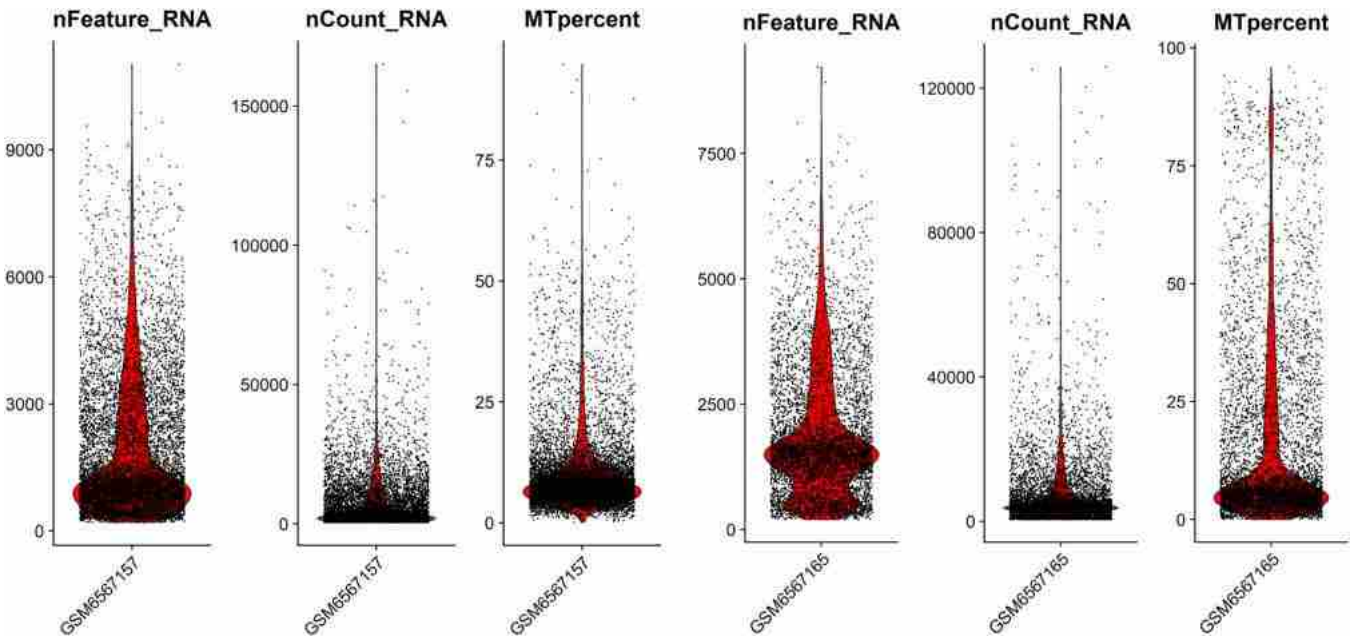

Fig. 1. Violin plots of gene number, count number and mitochondrial percentage in pancreatic ductal adenocarcinoma (A) and normal adjacent (B) sample. The dataset has been filtered out based on these violin plots.

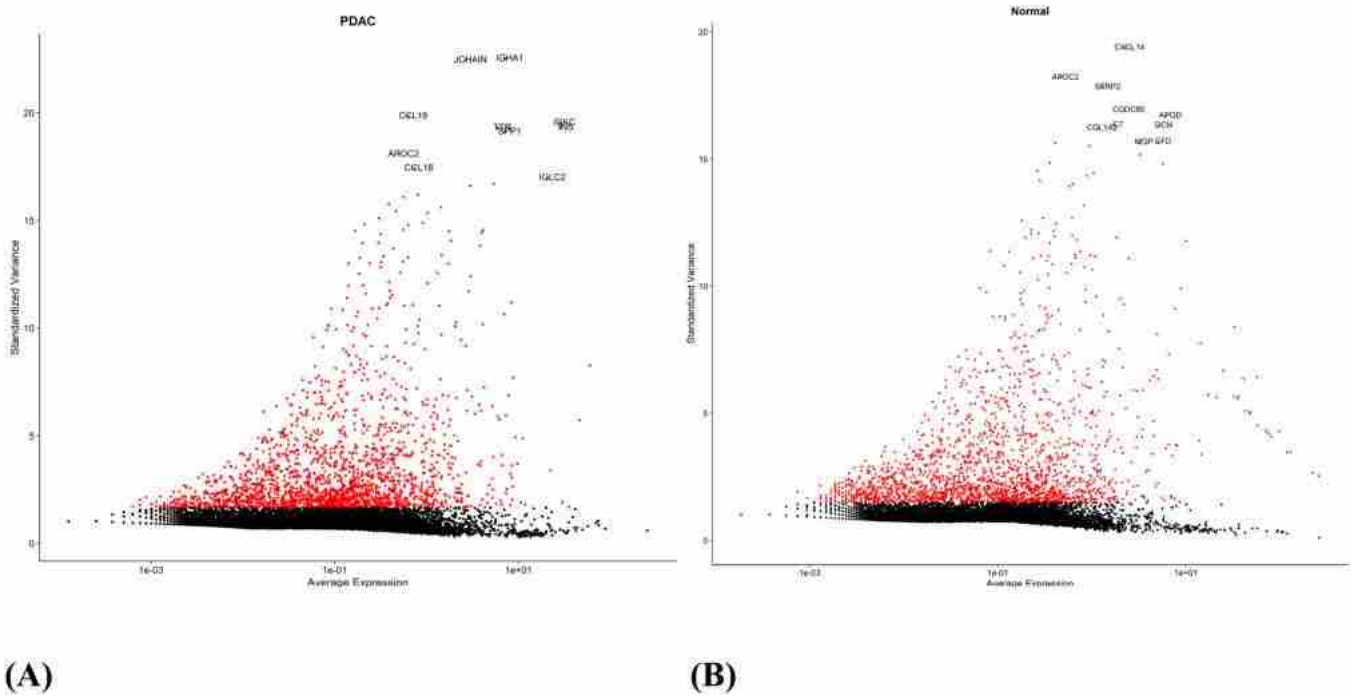

Fig. 2. Scatter plot of top variable genes in pancreatic ductal adenocarcinoma (A) and normal adjacent (B) sample. These plots display 10 top variable genes.

of this method in PDAC is limited by the low tumor cellularity and strong desmoplastic reactions in this type of cancer [3]. Therefore, single cell RNA-seq has been suggested as an influential technique for identification of the metabolic and clinical characteristics of this highly malignant tumor [3,9,11,27]. In the current study, we have analyzed single cell RNA-seq data with a systems biology approach to identify important differentially expressed genes in PDAC samples compared to adjacent non-cancerous samples.

2. Methods

2.1. Single cell RNA-seq data collection

To obtain the raw counts of single-cell RNA-seq data from GSE212966 (Illumina NovaSeq 6000 (Homo sapiens); GPL24676), consisting of 12 samples, we accessed the Gene Expression Omnibus (GEO; http://www.ncbi.nlm.nih.gov/geo/) on 18 November 2022. This dataset includes 6 PDAC and 6 adjacent normal pancreatic tissue samples. For our analysis, we specifically chose GSM6567157 as the PDAC sample and GSM6567165 as the adjacent normal pancreatic sample.

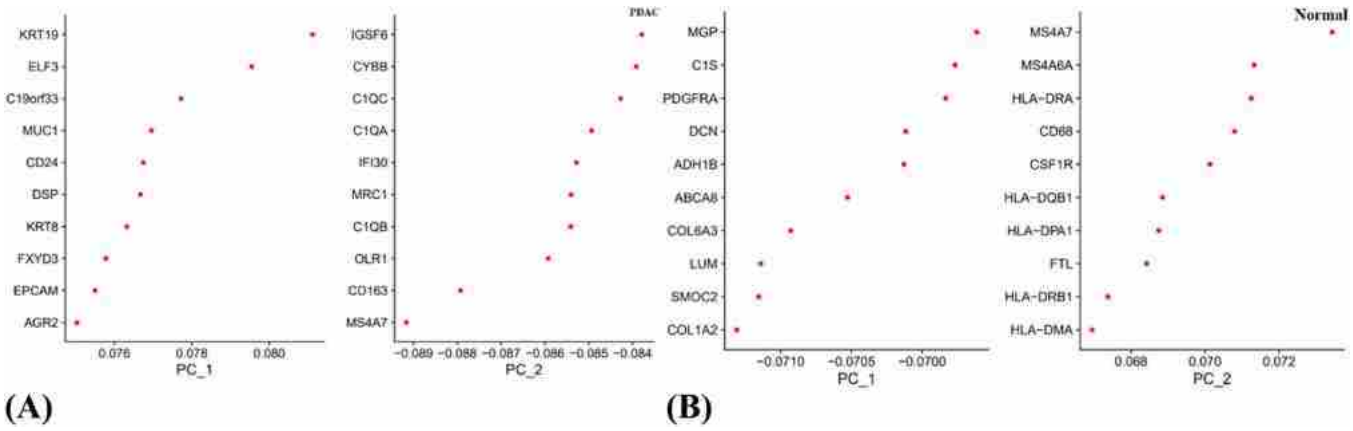

Fig. 3. Plots of top 10 genes in top two principal component in pancreatic ductal adenocarcinoma (A) and normal adjacent (B) sample.

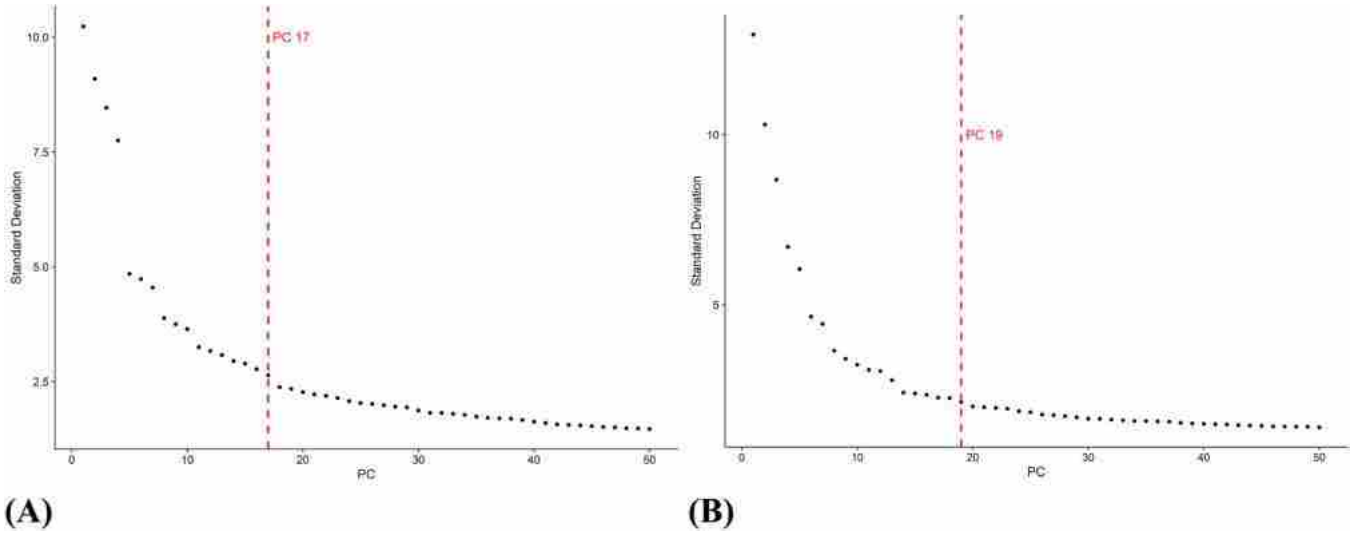

Fig. 4. Elbow plot for selecting the best principal components in pancreatic ductal adenocarcinoma (A) and normal adjacent (B) sample.

2.2. Data preprocessing and principal component analysis

The NormalizeData function of the Seurat package (version 4.1.1) [14] was used to normalize the expression matrix. Using the FindVariableFeatures function, the top 2000 highly variable genes were examined. The ScaleData function was then used to linearly scale the expression data. Finally, using the RunPCA function and the 2000 variable genes, principal component analysis (PCA) was carried out.

2.3. Cell cluster and annotation

We chose the primary components with high standard deviations. Then, using the FindNeighbors and FindClusters functions of the Seurat package, a cell clustering analysis was carried out. T-distributed Stochastic Neighbourhood Embedding (tSNE) and Uniform Manifold Approximation and Projection (UMAP) were used for dimension reduction through the use of the RunTSNE and RunUMAP functions. Then, after obtaining the markers for each cluster using the FindAllMarkers function, we set an average log2FC $> = 1$ threshold to choose the best markers. Based on the best marker genes, cell types were annotated. We utiliezed GenemarkeR [25], azimuth (https://azimuth.hubmapconsortium.org/), Tabula Muris [28], UNCURL (https://uncurl.cs.washington.edu/db_query) and Single Cell Expression Atlas [8] databases and also singleR package (Version 1.10.0) [2] to annotate clusters.

2.4. Dataset preprocessing, DEGs analysis and two-way clustering of DEGs

We used the DESeq2 package (version 1.36.0) [21] to analyze raw counts data, and the lfcShrink function and normal method to obtain DEGs. In addition, The P value was also converted into the FDR using Bonferroni in the stats package (version 4.2.1). We used the FDR < 0.05 and $|\log2\ FC = > 1$ as the cutoff criteria for DEGs between endothelial cells in PDAC and adjacent normal samples. Next, the whole list of lncRNA genes was obtained through approved HUGO Gene Nomenclature Committee (HGNC) symbols [33]. Next, we measured the levels of gene expression for important DElncRNA and DEmRNAs. In order to do the two-way clustering based on the Euclidean distance, we used this data in the pheatmap package of R programming language (version 1.0.12) [30].

2.5. Gene ontology (GO) enrichment analysis of DEGs

Gene ontology (GO) enrichment analysis was performed using the clusterProfiler R package (version 4.4.4) [36] to look into the roles of the substantially up- and down-regulated DEGs. The threshold for the functional category was set at an adjusted p-value of 0.05 or less.

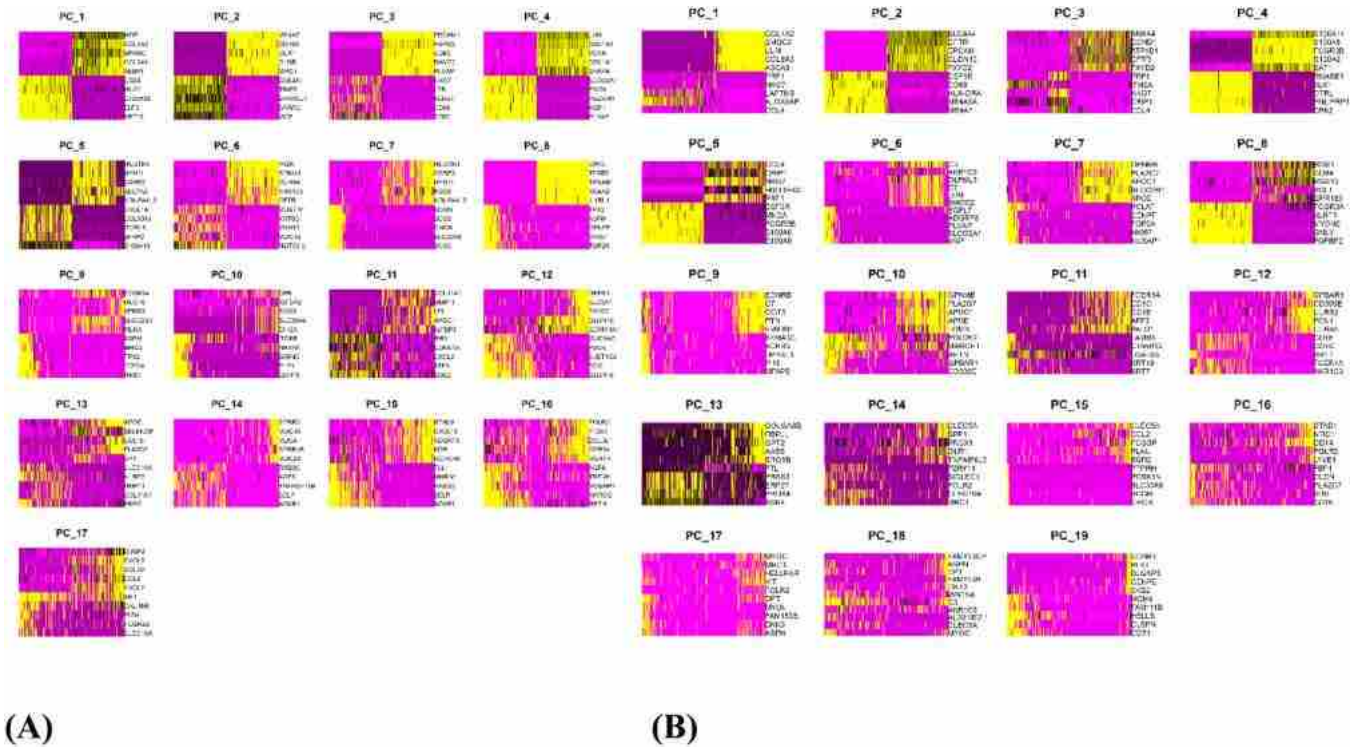

Fig. 5. Heatmaps showing the top 10 marker genes in each principal component in pancreatic ductal adenocarcinoma (A) and normal adjacent (B) sample.

2.6. Kyoto encyclopedia of genes and genomes (KEGG) pathway analysis

To determine the specific roles of DEGs engaged in the pathways based on the KEGG database [17], KEGG pathway analysis of DEGs was conducted. The threshold was set at a p-value of 0.05 or less.

2.7. Protein-protein interaction (PPI) network construction and hub genes identification

The PPI network for DEGs was constructed using the STRING database [32]. To construct the interactions parameters, the highest degree of confidence (confidence score > 0.9) and high FDR stringency (1%) were combined with experiments and database sources. The interactions between the proteins were viewed using the Cytoscape software version 3.9 [29]. Finally, utilizing the betweenness centrality methode and the Cytohubba plugin [7] of Cytoscape, the top 20 DEGs associated with hub genes were identified.

2.8. Regulatory Networks of miRNA-hub genes and TF-hub Genes

The connections between the PPI hub genes, transcription factors (TFs) and microRNAs (miRNAs) were developed using the NetworkAnalyst database [43]. We next determined which TF and miRNA had the highest degree in the networks.

2.9. Constructing the ceRNA networks and hub genes identification

We built a ceRNA network through the following steps: 1) Obtaining PDAC-related miRNAs from the miRCancer database [37]; 2) Finding the interaction between lncRNAs and miRNAs based on the PDAC-related miRNAs using miRcode (http://www.mircode. org/); 3) Application of miRDB (http://www.mirdb. org/) [6], miRTarBase (https://mirtarbase.cuhk.edu.cn/) [15], TargetScan (http://www.targetscan.org/) [1] and miRWalk (http://129.206.7.150/) [31] for prediction of miRNAs-targeted mRNAs; 4) Identifying the intersection of the differentially expressed lncRNAs and mRNAs, and constructing lncRNA/mRNA/miRNA ceRNA network using Cytoscape v3.9 and 4) predicting hub genes using cytohubba plugin based on degree method.

2.10. Validation of hub genes via expression values

The expression profile of the hub genes of the PPI and ceRNA networks in PDAC and healthy tissues was assessed using ualcan [4]. In this case, TCGA-PAAD data was chosen.

2.11. Survival analysis

We used ualcan database to generate survival curves, which were stratified by the patients' predictive value of hub genes with highest degree in PPI and ceRNA networks. The TCGA provided the clinical information for those with PDAC (TCGA-PAAD). Kaplan-Meier curves were used to evaluate univariate survival analyses. P-values < 0.05 were regarded as significant in statistics.

3. Results

3.1. Single cell RNA-seq dataset processing and clustering

Using the R package Seurat, we first downloaded the raw data for quality control and data filtering for the single-cell dataset GSE212966 and GSM6567157 and GSM6567165 samples. We filtered out cells based on count number, gene number and mitochondrial percentage that have been displayed in violin plots (Figs. 1A, 1B). We selected the top 2000 highly variable genes in each sample after normalizing the scRNA data (Figs. 2A and 2B). ScRNA data was then linearly scaled and analyzed using PCA to reduce dimensionality. We screened the top two principal components for further investigation (Figs. 3A and 3B). Based on the elbow point, we recognized the optimal principal components in PDAC

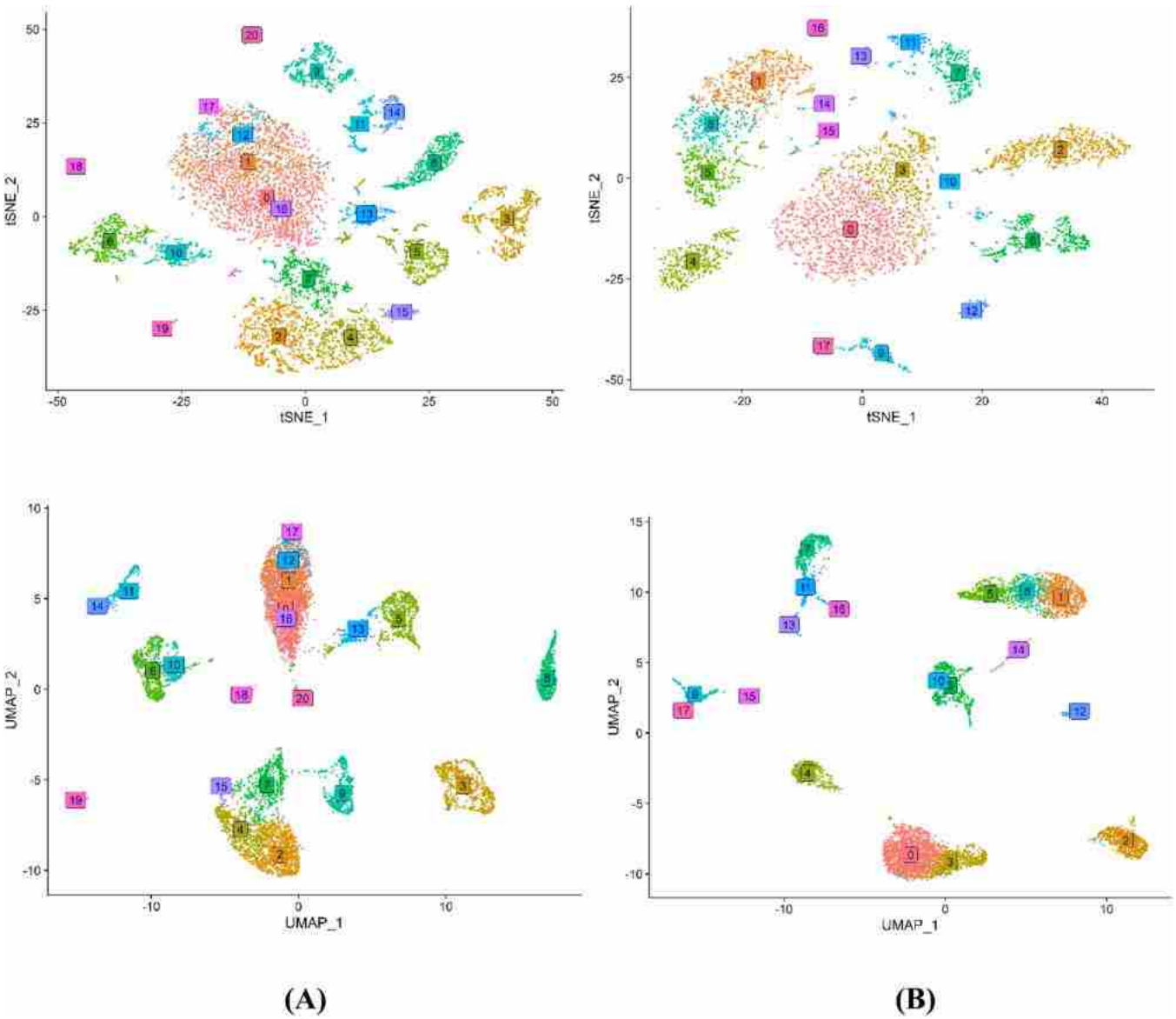

Fig. 6. Clustering based on tSNE and UMAP dimension reduction in pancreatic ductal adenocarcinoma (A) and normal adjacent (B) sample.

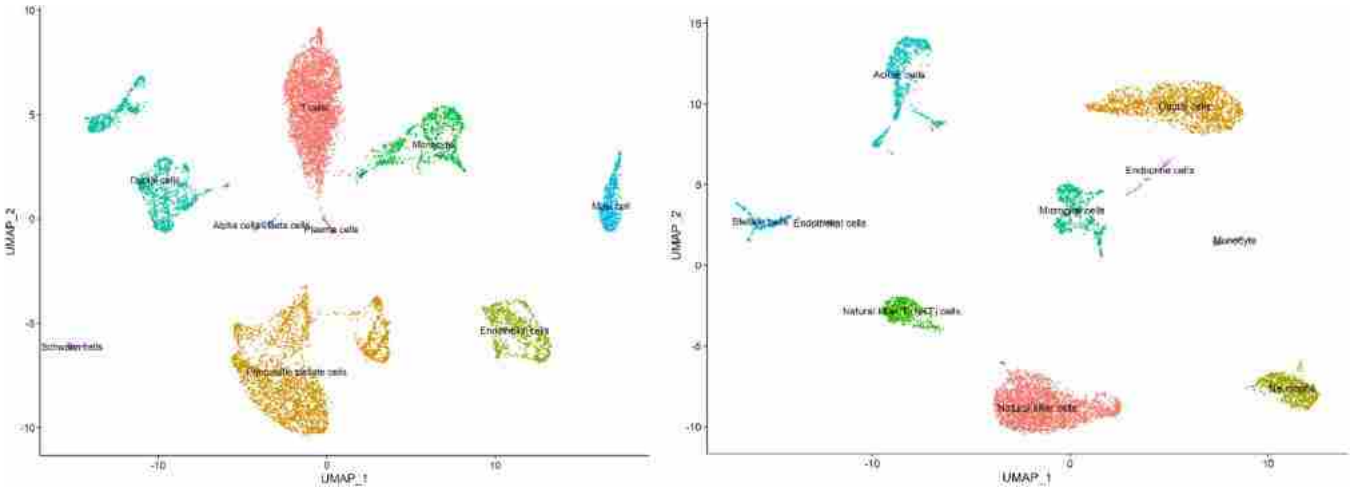

Fig. 7. UMAP plots demonstrating cell types recognized by marker genes. Each cell type was colored by a distinctive color in PDAC (A) and normal adjacent (B) sample using UMAP method.

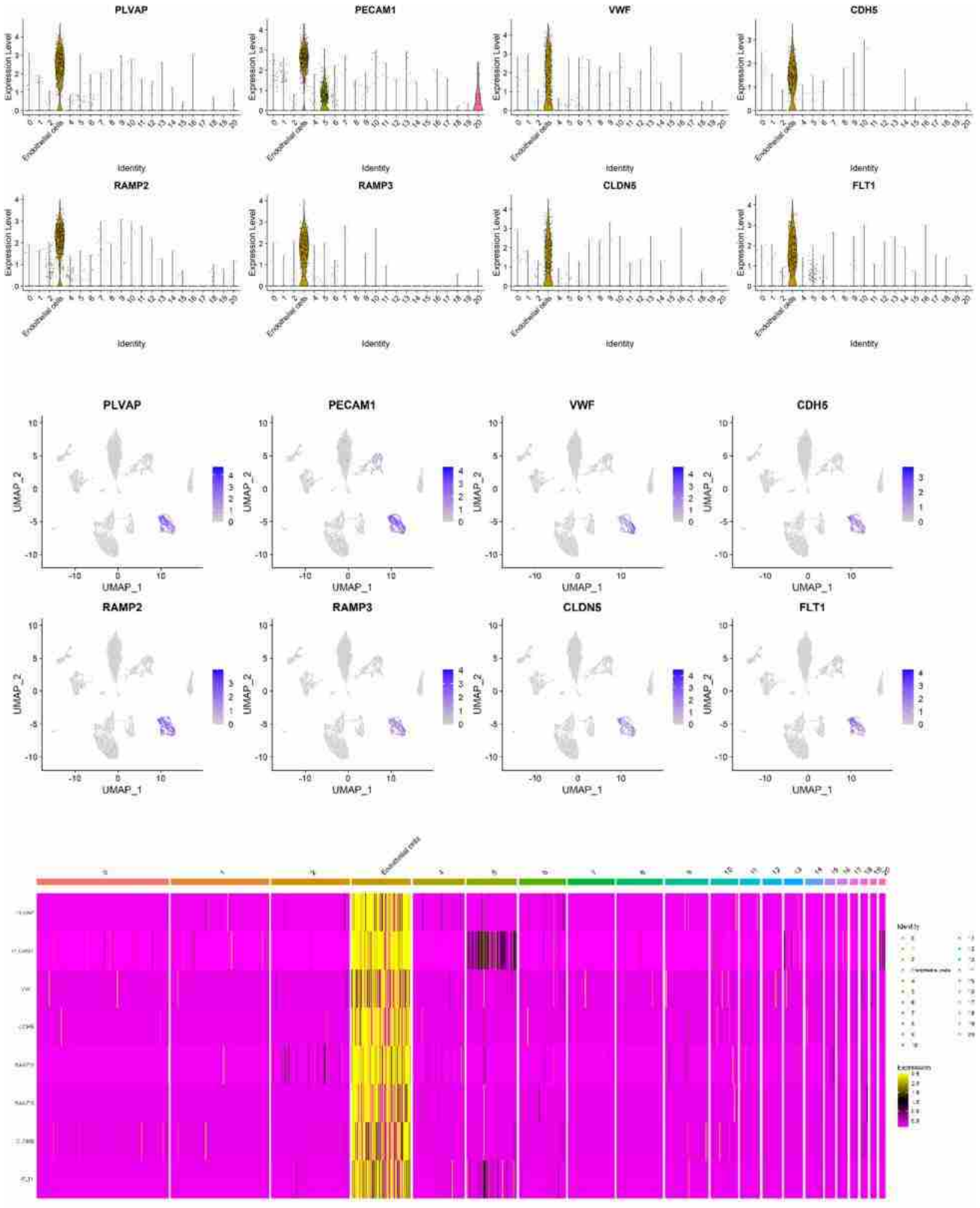

(A)

Fig. 8. Violin plot, feature plot and heatmap of 8 endothelial cell unique marker genes in pancreatic ductal adenocarcinoma (A) and normal adjacent (B) sample.

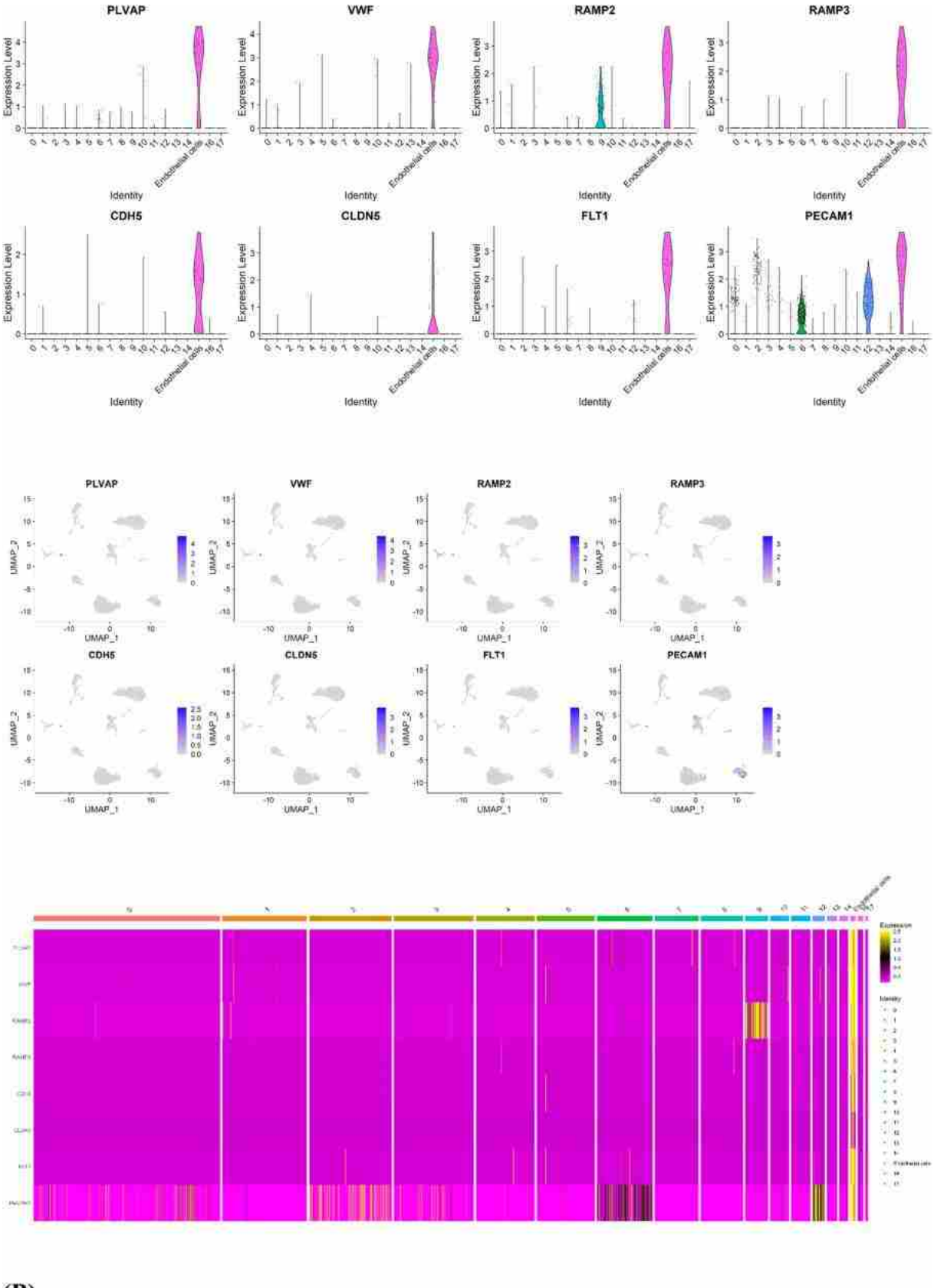

(B)

Fig. 8. (*continued*).

Table 1
The top 10 up- and downregulated DEmRNAs between PDAC and normal samples.

Down-regulated			Up-regulated		
DEmRNA	**Log FC**	**Adjusted *P* value**	**DEmRNA**	**Log FC**	**Adjusted P value**
PRSS1	-6.52532161684	0.000109758154973103	**HSPA1A**	3.22311028268	1.40812407296933e-12
CLPS	-6.37876537760	0.000452497346272236	**SOCS3**	2.63008472128	4.67310460777748e-10
CTRB1	-5.92073932417	0.00435285966419554	**FOSB**	2.62295638623	5.73171133382851e-10
PNLIP	-5.59818205342	0.00913875754383048	**LMNA**	2.62292614713	9.28518464180237e-12
CELA3A	-4.99493696351	0.00968701976717365	**JUNB**	2.33021819513	5.04910773521695e-09
FABP5	-4.88901122343	3.42938435789448e-47	**C11orf96**	2.28818983593	8.61685367604722e-05
CPA1	-4.86551713204	0.0396877209682425	**IGFBP5**	2.19485320295	0.00056205135512786
LIFR	-4.63543806465	7.52973647505902e-53	**MIDN**	2.17741775223	2.34909923104221e-07
CD36	-4.58160781574	3.02373171520527e-12	**IER3**	2.14319792434	1.10266740161394e-05
PRSS2	-4.48498316768	0.00603515779040049	**SLC2A3**	2.04979590162	1.26118994276069e-06

Table 2
The up- and downregulated DElncRNAs between PDAC and normal samples.

Down-regulated			**Up-regulated**		
DElncRNA	**Log FC**	**Adjusted *P* value**	**DElncRNA**	**Log FC**	**Adjusted P value**
LINC00472	-2.27381520663	6.87678108946863e-06	**SNHG5**	1.6625652117840	7.75249089978102e-06
SNHG7	-1.99167974598	8.09780009011294e-14			
LINC00342	-1.83568973995	0.00019503539112515			
MIRLET7BHG	-1.72711278714	0.00705657762480542			
MAPKAPK5-AS1	-1.49343425398	0.00446347247191309			
PSMB8-AS1	-1.47159920364	0.0126938151760183			
AC108134.3	-1.42422557735	0.0317427522947224			
LINC00667	-1.40852076207	0.00761175774901771			
MAP4K3-DT	-1.38960468297	0.0122715376278185			
LINC01278	-1.32491766312	0.0436713864832826			
CCDC18-AS1	-1.31517462665	0.0436713864832826			
AL390728.6	-1.30683815211	0.0298113889177917			
OTUD6B-AS1	-1.30320443121	0.00129179902407002			
WAC-AS1	-1.29394903246	0.0281810939950328			
GATA2-AS1	-1.29227301928	0.0253911669360233			
EBLN3P	-1.27463318009	0.00826503468046169			
AC005332.6	-1.26328138827	0.0137568279997822			
BX284668.5	-1.23064201116	0.0366268649533138			
HEIH	-1.20450179993	0.0403796332773609			
PHF1	-1.16260788551	0.0316204257893764			
SNHG14	-1.13553980662	0.0110210317274008			
ILF3-DT	-1.07585682081	0.0452350027780647			
NUTM2A-AS1	-1.06276252610	0.0107633557184179			
OIP5-AS1	-1.06203290673	0.0255665597172189			
LINC01116	-1.02748506731	0.0281810939950328			
FTX	-1.02183015464	0.00911212356827239			

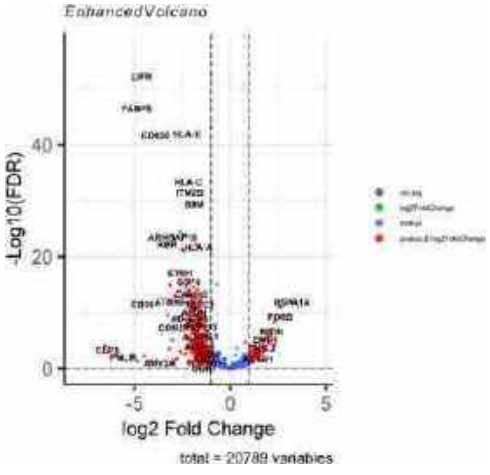

Fig. 9. The volcano plot of DEGs; horizontal axis, log_2(FC); vertical axis, $-log_{10}$(adjusted P value).

and normal sample as 17 and 19 respectively (Figs. 4A, 4B). Heatmaps depicted the top 10 marker genes in each principal component (Figs. 5A, 5B). With the UMAP and tSNE dimension reduction methods, PDAC and adjacent normal pancreatic samples were clustered into 21 and 18 clusters, respectively (Figs. 6A, 6B).

3.2. Identification of cell types and their marker genes across pancreatic endothelial cells

First, we identified marker genes in each cluster using FindAllMarkers function of Seurat package with average log2FC > 1 as a threshold. Then, we used GenemarkeR, azimuth, Tabula Muris, UNCURL and Single Cell Expression Atlas databases and also singleR package (version 1.10.0) to annotate each cell type (Figs. 7A and 7B). Pancreatic endothelial cell type was identified based on PLVAP, PECAM1, VWF, CDH5, RAMP2, RAMP3, CLDN5 and FLT1 gene markers (Figs. 8A and 8B). Also, considering that most of the pancreatic tissues examined in these databases included pancreatic islets, the endothelial cells are also in the form of islet endothelial cells.

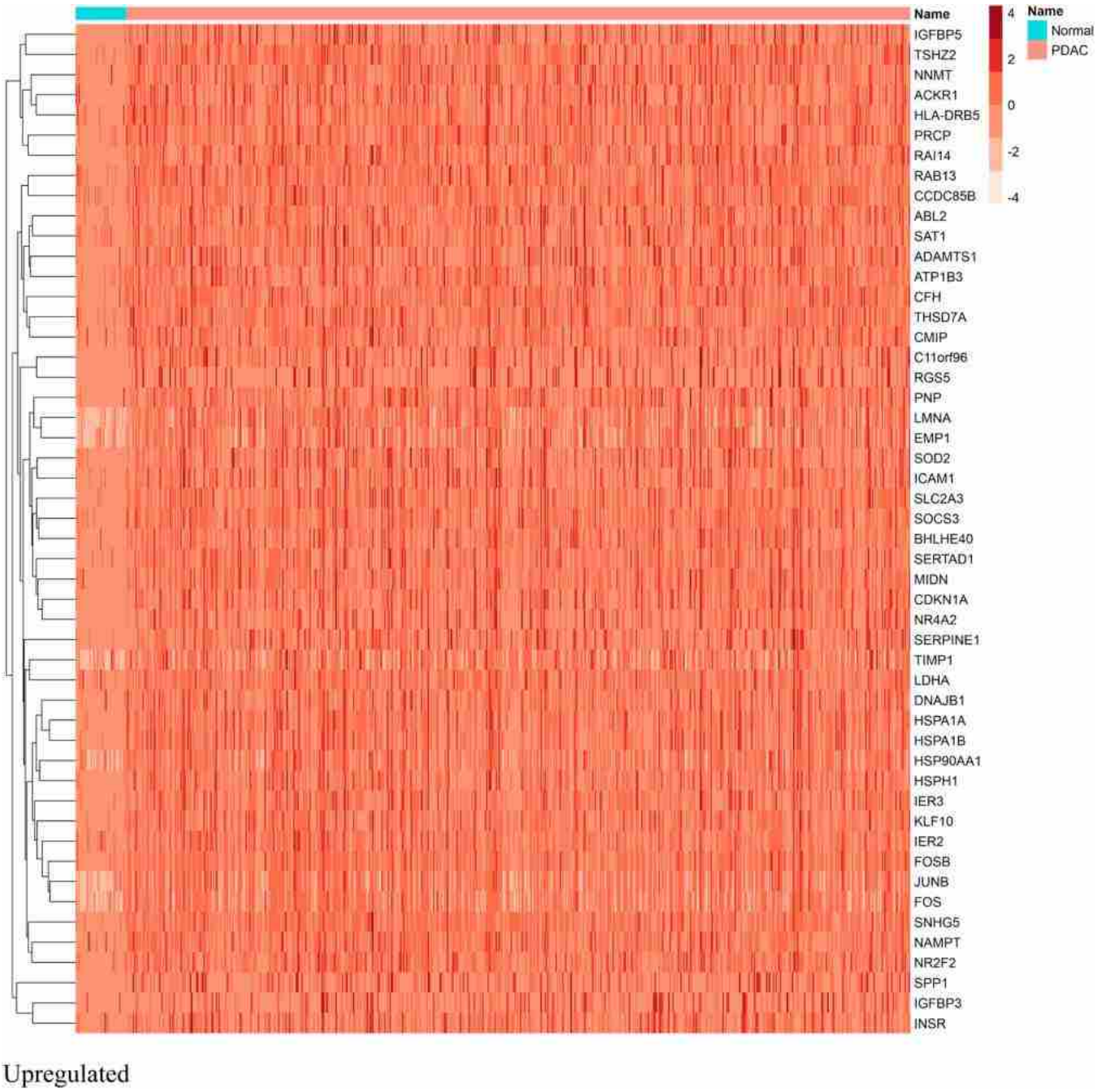

Fig. 10. The two-way clustering of DEmRNAs between endothelial cells of PDAC and endothelial cells of normal samples; horizontal axis, the samples; vertical axis, DEmRNAs.

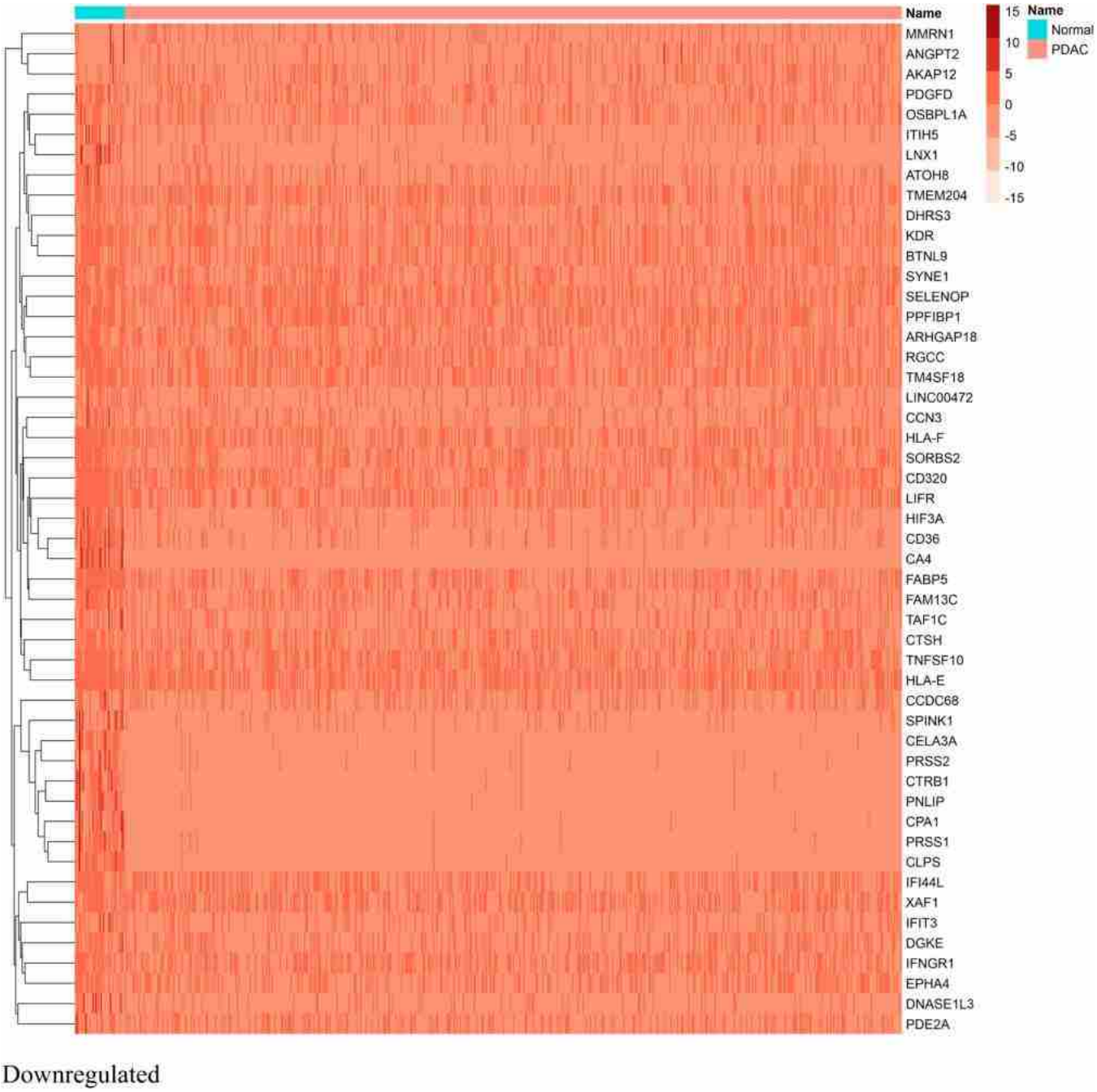

Fig. 10. (*continued*).

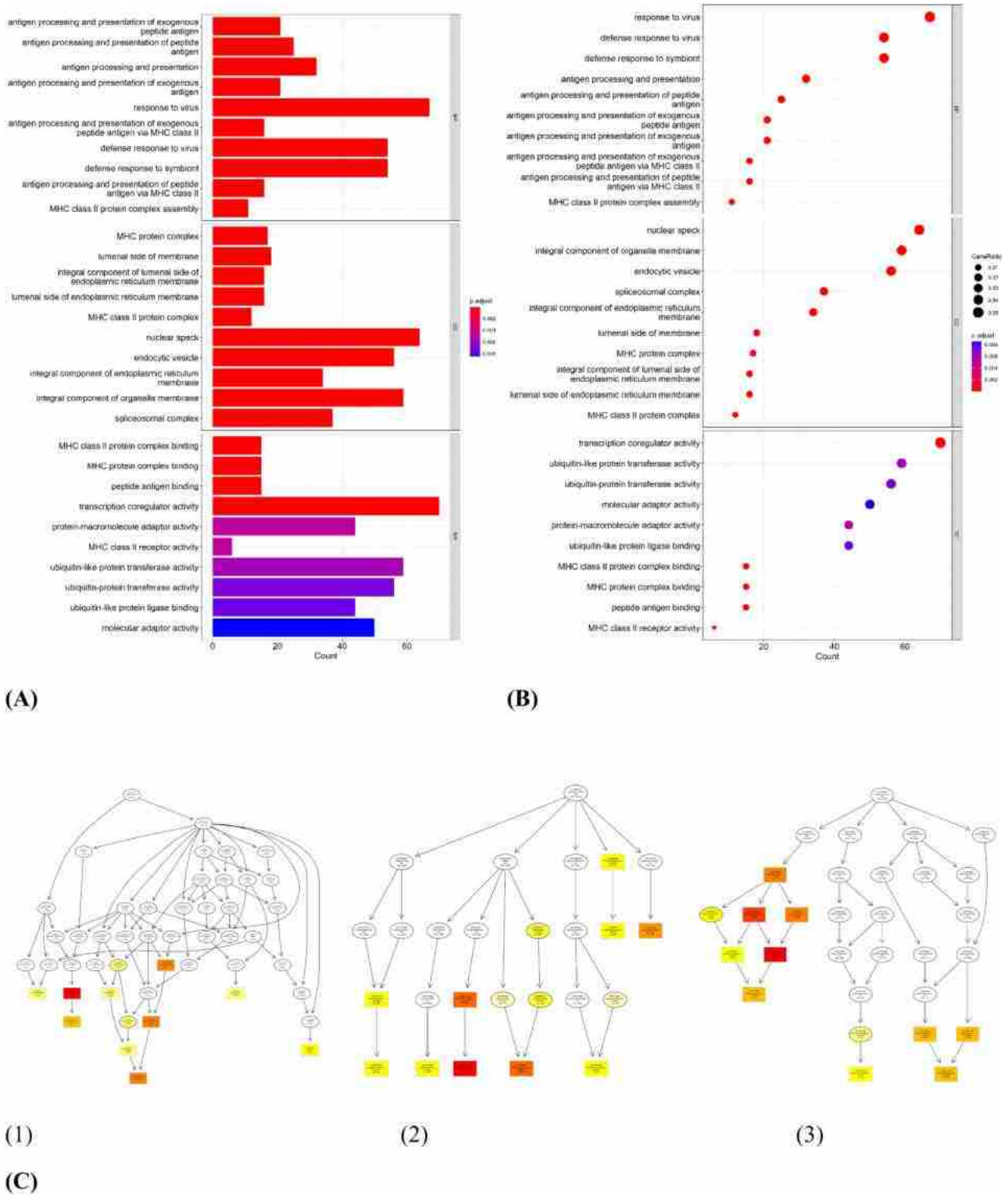

Fig. 11. The plots related to the analysis of gene ontology (GO) enrichment. A) The top 10 enriched functions are displayed as a bar plot, with the geneset count on the x-axis and the geneset function on the y-axis. The color of the bar represents the adjusted P.value, ranging from red (most significant) to blue (least significant). B) The top 10 enriched functions are shown as a dot plot, with the geneset count on the x-axis and the geneset function on the y-axis. The color of the dot reflects the adjusted P.value, ranging from dark blue (most significant) to red (least significant). The size of the dot indicates the GeneRatio, increasing as the gene ratio increases. C) The top GO terms are presented as a GO graph visualization, with sub-graphs created using the top 10 GO terms in the "Cellular Component," "Molecular Function," and "Biological Process" categories. Significant terms are highlighted in colored boxes, ranging from dark red (most significant) to light yellow (least significant). D) The top 5 GO terms are visualized as a network, with the size of the dot representing the number of genes associated with the GO term. The genes are connected to the associated GO term with a distinctive color. E) An UpSet plot is used to represent subsets of 10 GO terms, with dots and lines showing the relationships between them.

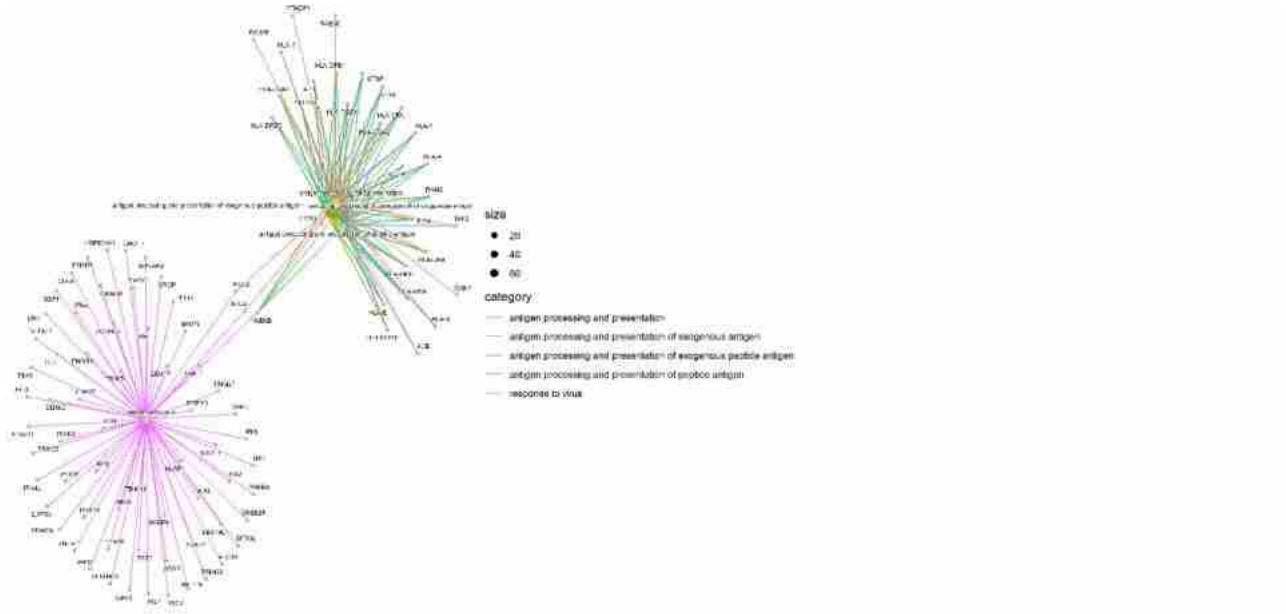

(D)

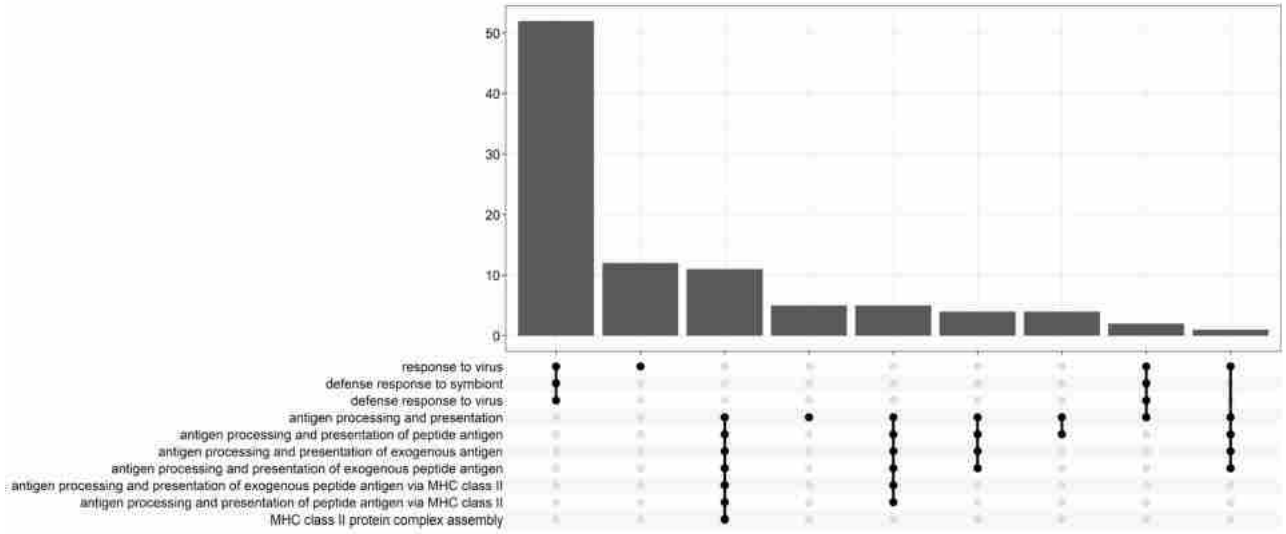

(E)

Fig. 11. (*continued*).

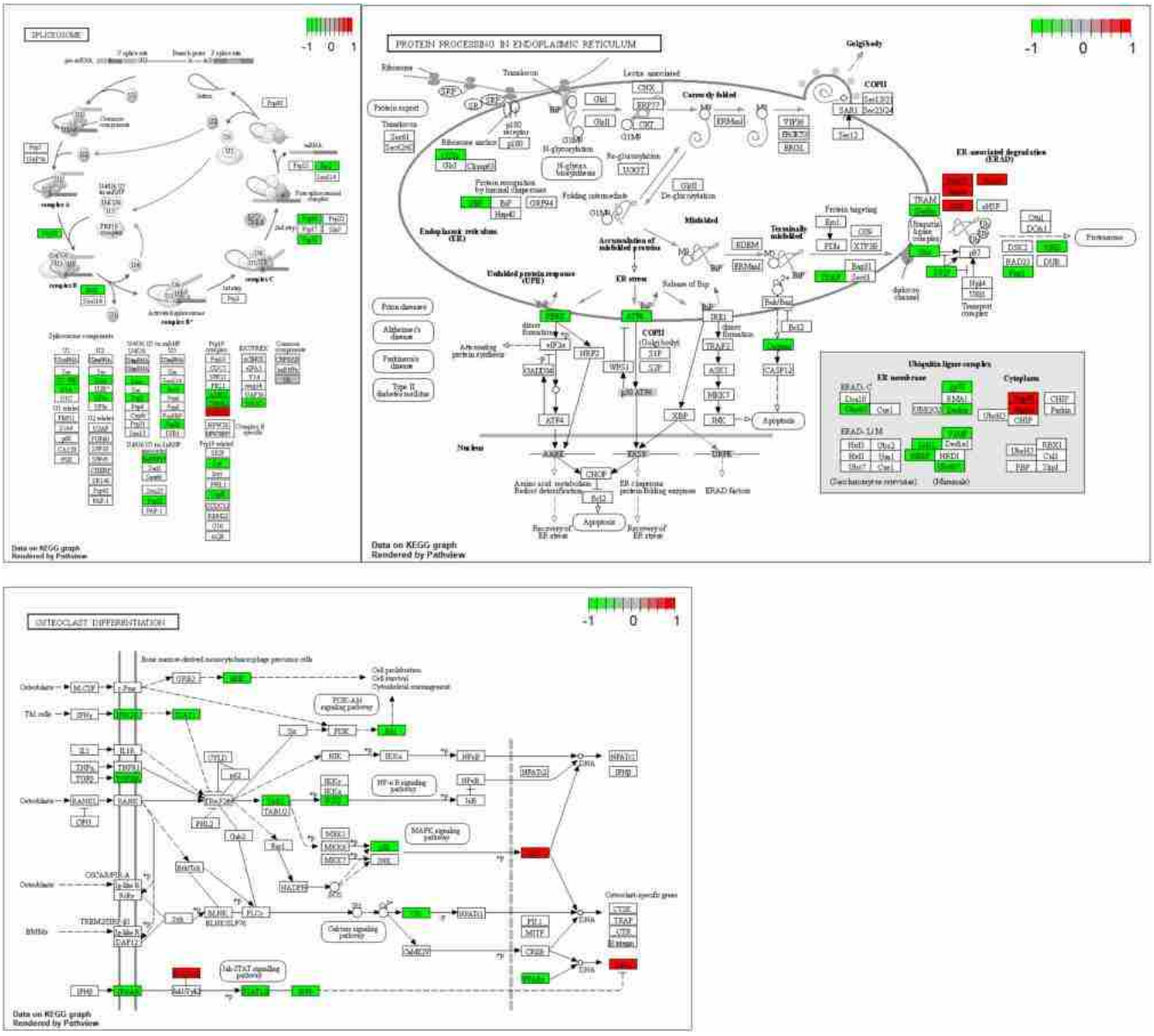

Fig. 12. Three upregulated pathways are visualized. genes that are upregulated are shown by red boxes and downregulated by green boxes.

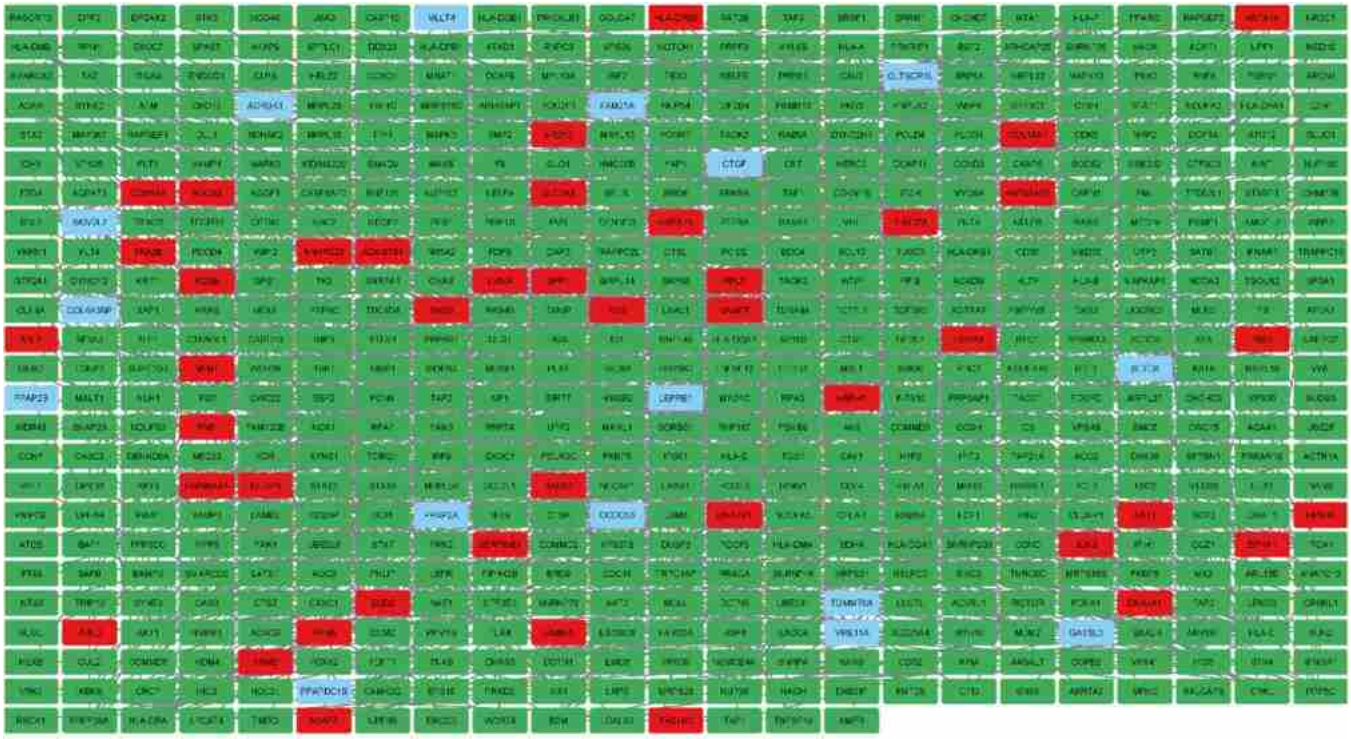

(A)

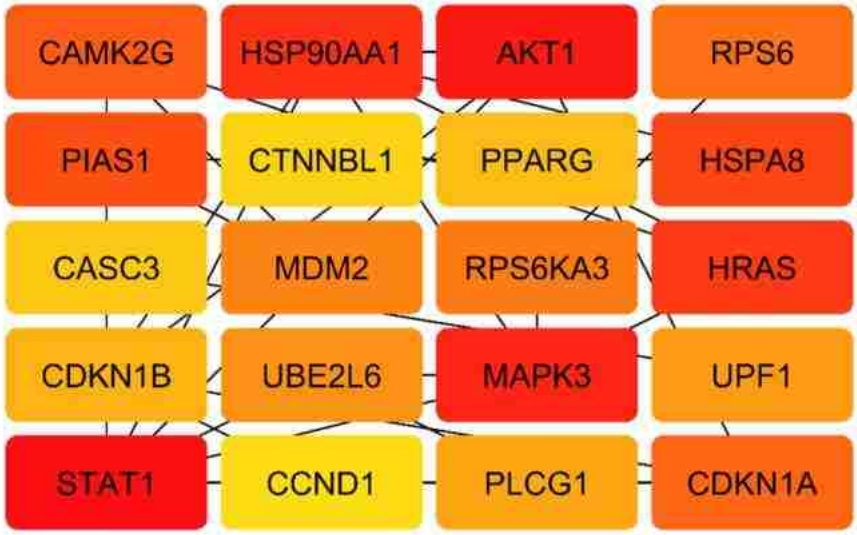

(B)

Fig. 13. PPI network of DEmRNAs. A) Total PPI network, B) Subnetwork of hub genes.

Table 3
Information about the PPI network's hub genes.

Hub Gene	Clustering Coefficient	Degree	Closseness Centrality	Betweenness Centrality
STAT1	0.37471264367816093	30	0.30758524704244955	0.21163987468166265
AKT1	0.11462450592885376	23	0.2998643147896879	0.1795588242960587
MAPK3	0.10294117647058823	17	0.2960482250502344	0.16270832980448133
HSP90AA1	0.1568627450980392	18	0.30694444444444446	0.1478725270758565
HRAS	0.036923076923076927	26	0.28117048346055984	0.14363173624104197
HSPA8	0.1111111111111111	18	0.2535857716580608	0.13203852675424355
PIAS1	0.0	12	0.2610750147666863	0.07184884221214391
CAMK2G	0.022222222222222223	10	0.2672309552599758	0.07112843954762078
CDKN1A	0.2571428571428571	15	0.28188775510204084	0.07091765454549095
RPS6	0.4666666666666667	10	0.1930131004366812	0.06784306127029646
RPS6KA3	0.0	2	0.23312236286919832	0.06772750833361509
MDM2	0.11764705882352941	17	0.26967663209273945	0.06719352769762318
UBE2L6	0.14102564102564102	13	0.2629387269482451	0.06601242969573037
UPF1	0.3	5	0.21762678483505662	0.06394331203590689
PLCG1	0.12380952380952381	15	0.23177766124803356	0.05790741569410645
CDKN1B	0.24761904761904763	15	0.27133210558624926	0.05632434224413924
PPARG	0.06666666666666667	6	0.23312236286919832	0.05366431350962938
CASC3	0.2857142857142857	7	0.18264462809917356	0.05328888512766141
CTNNBL1	0.0	2	0.20731707317073172	0.050995010945633315
CCND1	0.175	16	0.2556390977443609	0.04797144469337734

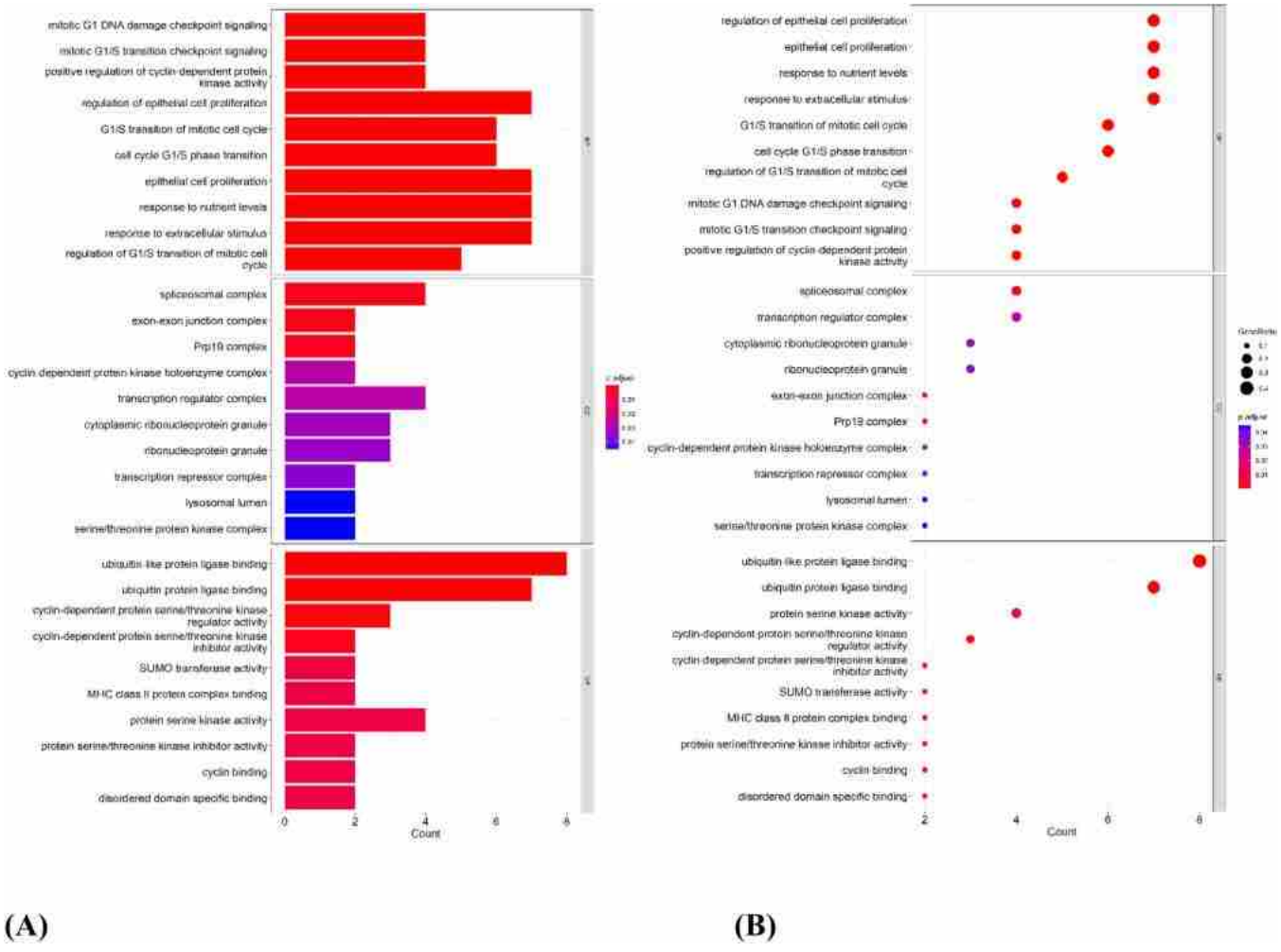

Fig. 14. Analysis of functional enrichment for hub genes. Bar plot and Dot plot of enriched GO terms showing hub genes.

3.3. DEGs Analysis

Using the DESeq2 package (version 1.36.0), we analyzed the endothelial cells count matrix from PDAC and adjacent normal samples, resulting in the identification of 1462 DEmRNAs, consisting of 1389 downregulated DEmRNAs (such as PRSS1 and CLPS) and 73 upregulated DEmRNAs (such as HSPA1A and SOCS3), as well as 27 DElncRNAs, comprising of 26 downregulated DElncRNAs (such as LINC00472 and SNHG7) and 1 upregulated DElncRNA (SNHG5) (Tables 1 and 2).

We utilized the EnhancedVolcano package [20] in R to produce the

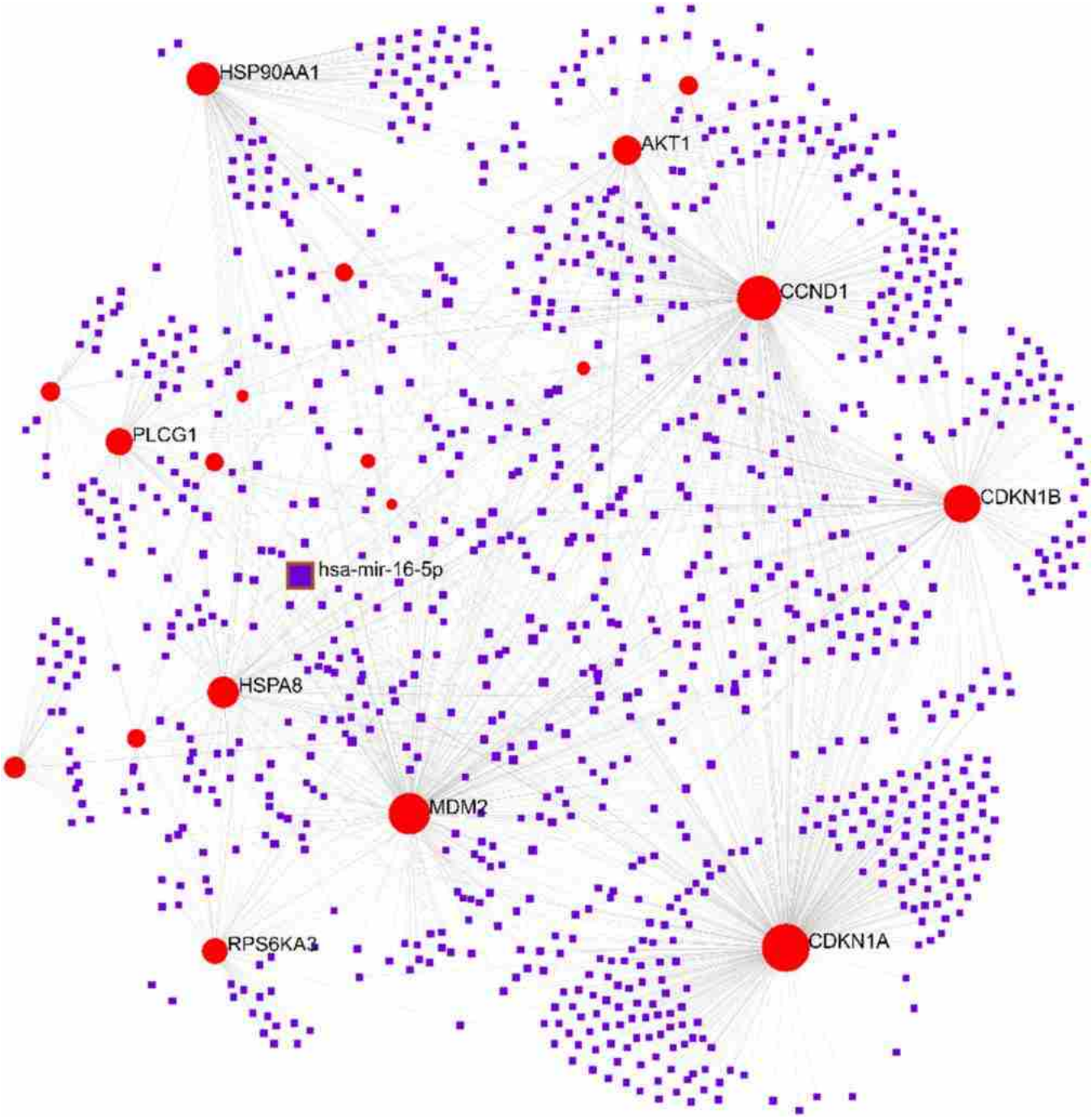

Fig. 15. Top 19 hub genes in the integrated miRNA-DEGs network. The 19 hub genes are represented by red circles, while miRNAs are represented by purple squares in the integrated miRNA-DEGs network shown in Fig. 15. A purple square with a red border is used to indicate miRNA with high connective properties to the hub genes.

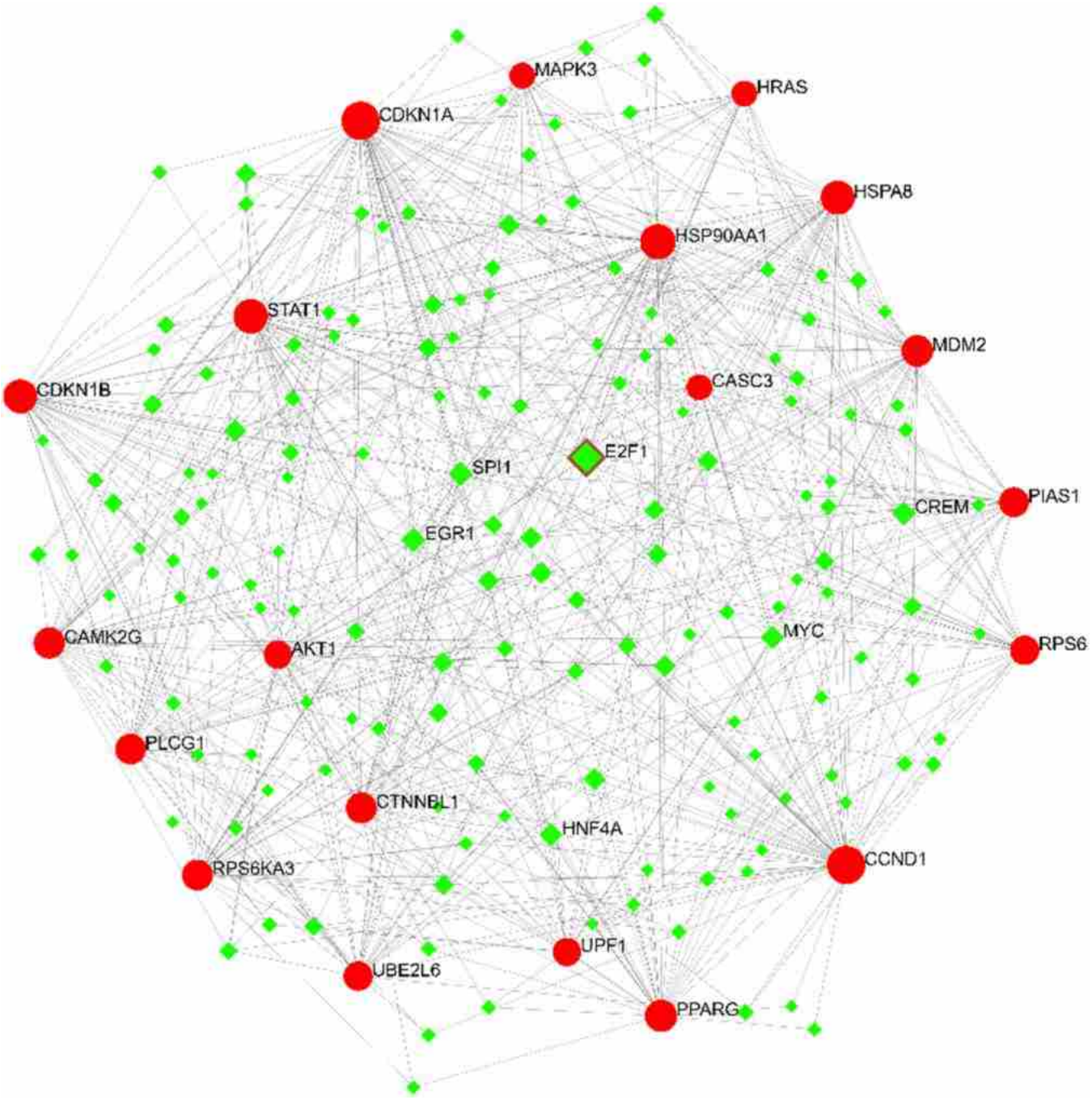

Fig. 16. The network of TF-hub genes. Circles show the hub genes, while the diamonds represent TFs targeting the hub genes. The green diamond with red border indicates TF with high connective properties to the hub genes.

Table 4
The interaction between 6 DElncRNAs, 13 DEmiRNAs and 32 mRNAs in ceRNA network.

lncRNA	miRNA	mRNA
SNHG5	hsa-miR-150	NR2F2
LINC00324, OIP5-AS1, SNHG14	hsa-miR-27b	EML1, NR5A2
LINC00324, OIP5-AS1, SNHG14	hsa-miR-27a	YAP1, SPATA13, TGOLN2, NF1, LIFR
LINC00324, SNHG14,	hsa-miR-31	RASA1
OIP5-AS1, PHF1, SNHG14, SNHG7	hsa-miR-107	RUNX1T1, OGT, SNCG, PPP6C, UBR3, PRR14L, NF1
OIP5-AS1, SNHG14	hsa-miR-30b-5p	ZDHHC17
OIP5-AS1, SNHG14	hsa-miR-21	PAN3, SATB1, NFIB
OIP5-AS1, PHF1, SNHG14	hsa-miR-212	POGZ, MECP2
OIP5-AS1	hsa-miR-196a	CPD
OIP5-AS1, PHF1, SNHG14, SNHG7	hsa-miR-34a	CDK6, POU2F1, ANKS1A, PPP1R11, MDM4, ZC3H4
OIP5-AS1, SNHG14, SNHG7	hsa-miR-18a	PNISR, STK4
OIP5-AS1, PHF1, SNHG14	hsa-miR-194	ITGA9
PHF1, SNHG14	hsa-miR-125a-5p	LIFR, ADAM9

volcano plot that facilitated the analysis of discrepancies in mRNA and lncRNA expression in PDAC and normal samples (Fig. 9). Furthermore, our analysis demonstrated that we could discriminate 50 DEmRNA expression patterns that were significantly different between normal and PDAC samples using two-way clustering (Fig. 10).

3.4. Gene ontology (GO) enrichment analysis of DEGs

Our analysis of differentially expressed genes (DEGs) utilized the clusterProfiler package to conduct gene ontology enrichment. To establish a background for our analysis, we utilized all the genes present in the clusterProfiler database. Our results yielded a total of 352 GO entries, where the majority of these entries were associated with biological processes (BP), followed by cellular component (CC) and molecular function (MF). All of these entries satisfied an Adjusted P value of less than 0.05. Totally, 265 of these terms are related to BP, 58 to CC, and 29 to MF. The first 15 entries were MHC protein complex (CC), antigen processing and presentation of exogenous peptide antigen (BP), antigen processing and presentation of peptide antigen (BP), lumenal side of membrane (CC), antigen processing and presentation (BP), antigen processing and presentation of exogenous antigen (BP), integral component of lumenal side of endoplasmic reticulum membrane (CC), lumenal side of endoplasmic reticulum membrane (CC), MHC class II protein complex (CC), response to virus (BP), antigen processing and presentation of exogenous peptide antigen via MHC class II (BP), defense response to virus (BP), defense response to symbiont (BP), MHC class II protein complex binding (MF) and antigen processing and presentation of peptide antigen via MHC class II (BP). Fig. 11A and 11B display the top 10 enriched functions using a barplot and a dotplot, respectively. Fig. 11C provides a visualization of the enriched Gene Ontology (GO) induced graph, while Fig. 11D presents the gene-concept network for the top 5 GO terms, including antigen processing and presentation, antigen processing and presentation of exogenous antigen, antigen processing and presentation of exogenous peptide antigen, antigen processing and presentation of peptide antigen, and response to virus. Fig. 11E, on the other hand, illustrates the intersection between the top 10 GO terms using an UpSet plot. This plot showcases the gene overlap between several gene sets.

3.5. Kyoto encyclopedia of genes and genomes (KEGG) pathway analysis

To find the probable functional genes, KEGG pathways analysis of 1389 DEGs with lower expression and 73 DEGs with higher expression were conducted in R using the pathview (Version 1.36.1) [22] and gage (Version 2.46.1) [23] packages. As a result, three pathways, including Protein processing in endoplasmic reticulum, Osteoclast differentiation, MAPK signaling pathway and Spliceosome, were obtained from pathway analysis with P-value less than 0.05, and all three of these pathways were upregulated in PDAC samples compared to normal samples (Fig. 12).

3.6. PPI network construction and assortment of hub genes

To identify the hub genes in the PPI network of DEGs (Fig. 13A), which consisted of 567 nodes and 1308 edges and was generated by the STRING, we used the Cytohubba plugin of Cytoscape 3.9 (Fig. 13B). The top 20 hub genes with the highest connectivity degree were identified and included CAMK2G, HSP90AA1, AKT1, RPS6, PIAS1, CTNNBL1, PPARG, HSPA8, CASC3, MDM2, RPS6KA3, HRAS, CDKN1B, UBE2L6, MAPK3, UPF1, STAT1, CCND1, PLCG1, and CDKN1A. Table 3 provides information on these hubs, which are ranked in order from the greatest degree of connectivity to the lowest.

3.7. Analysis of hub genes

The analysis of functional enrichment showed that there were 20 main hub genes in the PPI network, which were mostly related to biological processes like signaling for DNA damage checkpoint and G1/S transition checkpoint in mitosis, promotion of cyclin-dependent protein kinase activity, regulation of epithelial cell proliferation, and G1/S transition of mitotic cell cycle. This information is presented in Fig. 14A and B.

3.8. Examination of the regulatory network of miRNA-hub genes

MiRNAs have diverse functions in regulating gene expression. The Networkanalyst online database was used to gather miRNAs that target hub genes (shown in Fig. 15), and the miRTarBase v8.0 database was utilized to identify hub-miRNA interactions. Interestingly, all the hub genes, except for UBE2L6, were found to be associated with miRNAs. Among them, Hsa-miR-16–5p had the highest level of interaction with the hub genes (degree 7), indicating that it could play a significant role in the development of PDAC.

3.9. Examination of the regulatory network of TF-hub genes

We obtained TF's targeting hub genes from the NetworkAnalyst database (Fig. 16) and we chose ChEA database to discover the TFs that targets the hub genes. The TF-hub gene network showed that the E2F1 regulates 15 hub genes and can be crucial for the development of PDAC.

3.10. ceRNA network construction in PDAC

As per the theory of ceRNA, it is proposed that lncRNA might act as an endogenous sponge and regulate mRNA production by sequestering miRNA [13]. To create the lncRNA-miRNA-mRNA ceRNA network, the researchers considered miRNAs that showed upregulation or downregulation, as well as lncRNAs or mRNAs with reverse associations with miRNAs in the miRNA-mRNA and lncRNA-miRNA interaction pairs [39]. To identify miRNAs related to pancreatic ductal adenocarcinoma (PDAC), we searched the miRCancer database using the specific phrase "pancreatic ductal adenocarcinoma". Next, we utilized miRcode to examine the link between lncRNAs and miRNAs, which showed that

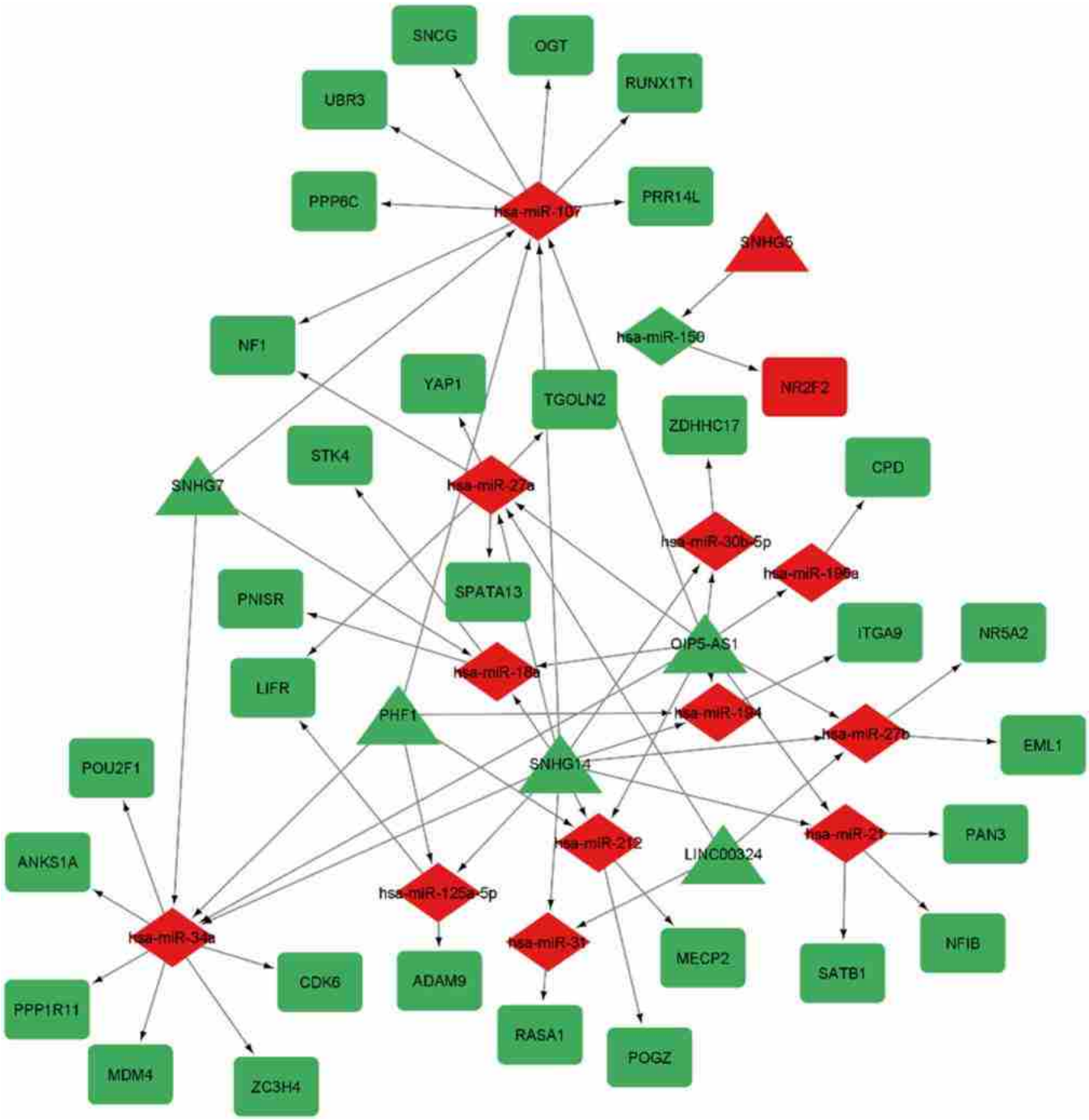

Fig. 17. CeRNA network in PDAC endothelial cells. Green nodes represent a low level of expression, whereas red nodes represent a significant level of expression. Protein-coding genes are shown by round rectangles, miRNAs are represented by diamonds, lncRNAs are represented by triangles, and interactions between lncRNAs, miRNAs, and mRNA are indicated by gray edges.

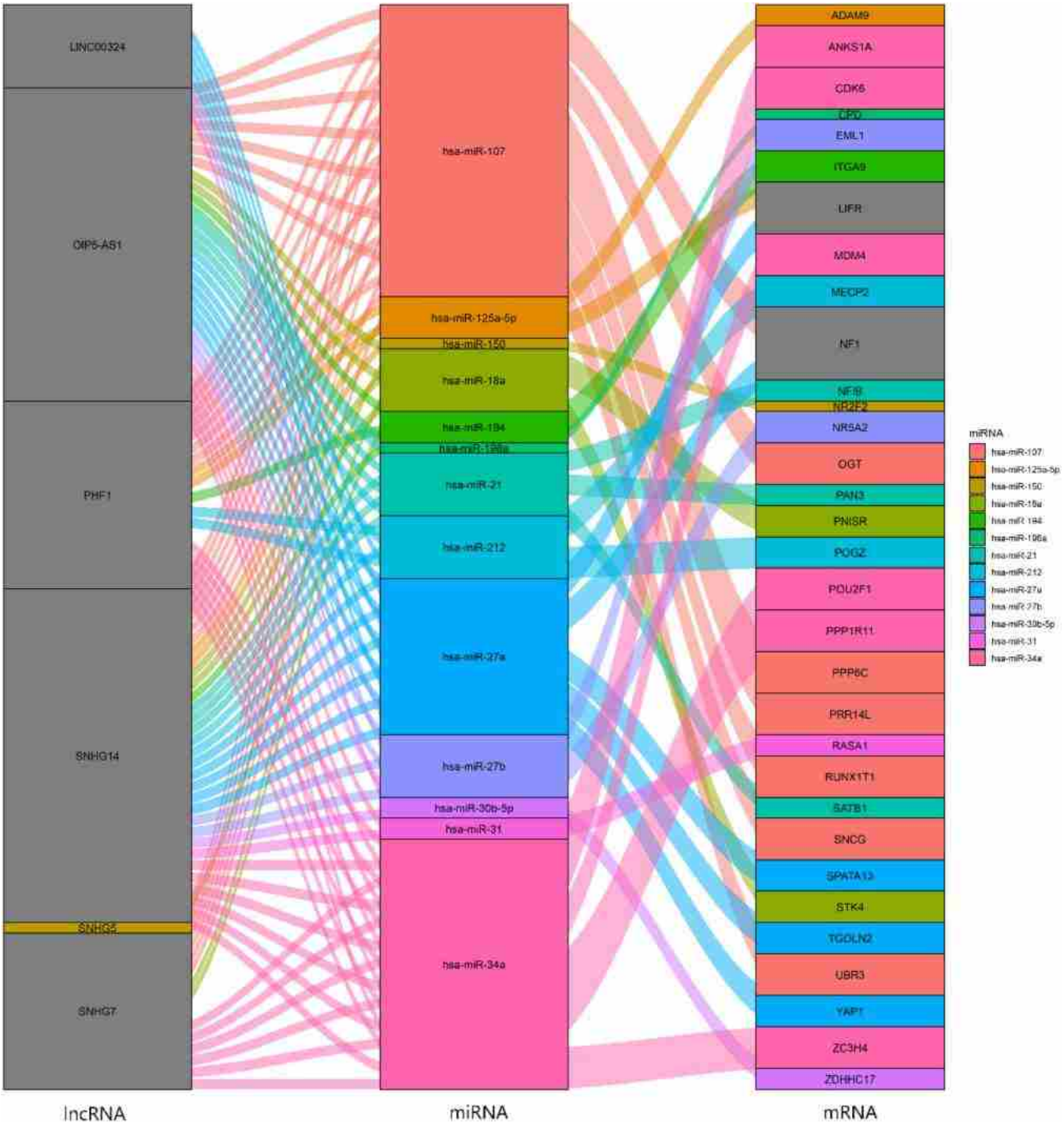

Fig. 18. Using a Sankey diagram, the ceRNA network in PDAC endothelial cells is shown. Each rectangle signifies a gene, and the degree of interaction between each gene is designated by the size of the rectangle.

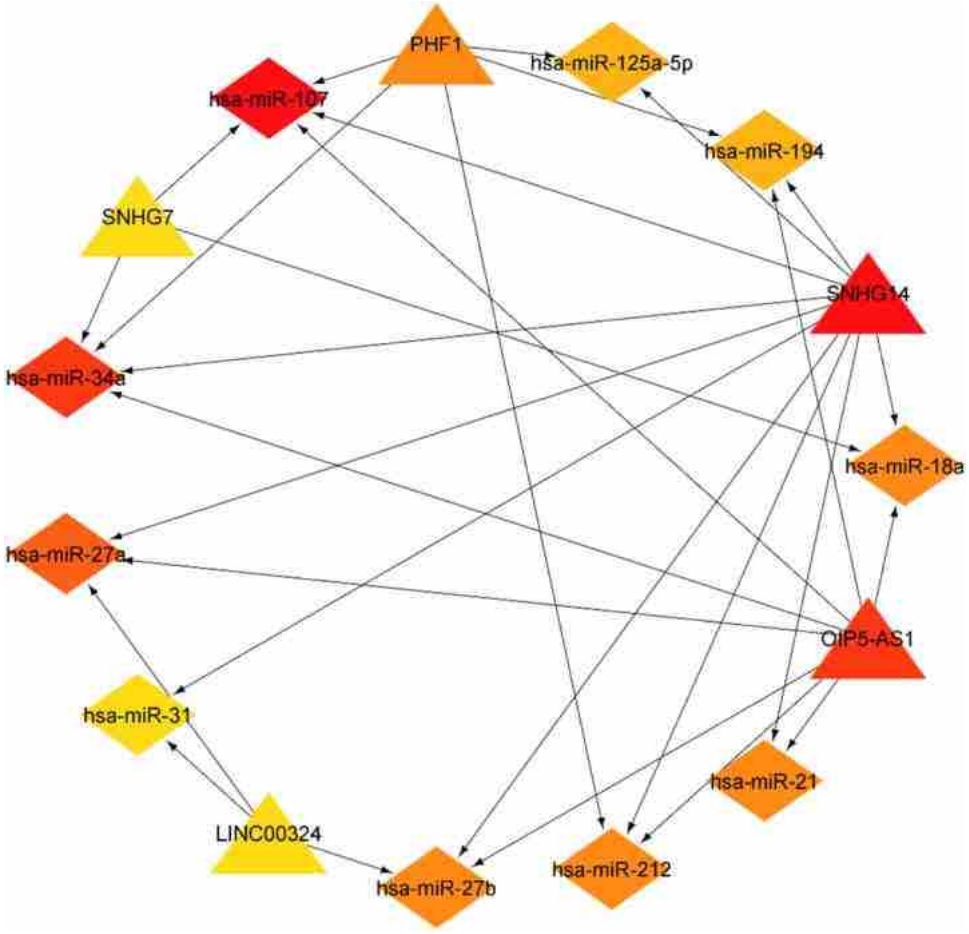

Fig. 19. Top 15 genes with highest degree centrality in ceRNA network.

eight of the 27 DElncRNAs might target 51 out of the 77 PDAC-specific miRNAs. We then employed miRWalk with miRTarBase, TargetScan, and miRDB filters, with a 0.95 confidence interval and 1% FDR stringency, to determine the mRNAs that were targeted by these 51 miRNAs. After analyzing the data, we identified 32 miRNAs that are linked to PDAC and may target 299 of the 1482 mRNAs. To refine our results, we removed any miRNA-targeted mRNA that was not present in the differentially expressed mRNAs (DEmRNAs). Additionally, any connection between lncRNAs and miRNAs, as well as miRNAs and mRNAs, that showed an opposite expression pattern was removed in accordance with the ceRNA network theory. The final ceRNA network consisted of six lncRNAs, 13 miRNAs, and 32 mRNAs, and is detailed in Table 4. We utilized Cytoscape 3.9 to construct a ceRNA network comprising 13 miRNAs, 6 lncRNAs, and 32 mRNAs, as illustrated in Fig. 17. Our aim was to explore the effects of lncRNAs on mRNAs in PDAC through their interactions with miRNAs. To present these interactions in a comprehensive manner, we generated a Sankey diagram employing the ggalluvial R package (version 0.12.3) [18], which is depicted in Fig. 18. The Sankey diagram visualizes the relationships between lncRNAs, miRNAs, and mRNAs in the ceRNA network, providing an intuitive and concise representation of the data. The top 15 nodes in the network with the highest degree centrality were displayed after we calculated nodes degree centrality using the cytohubba plugin (Fig. 19). As 15 hub genes in the ceRNA network, we identified SNHG14, OIP5-AS1, PHF1, LINC00324, SNHG7, hsa-miR-107, hsa-miR-125a-5p, hsa-miR-194, hsa-miR-18a, hsa-miR-21, hsa-miR-212, hsa-miR-27b, hsa-miR-27a, hsa-miR-31 and hsa-miR-34a.

3.11. Validation of hub genes via expression value

The ualcan tool was used to assess the expression level of hub genes in both PPI and ceRNA networks. The analysis revealed that CCND1, CDKN1B, MAPK3, PLCG1, and PPARG showed strong statistical significance. These findings are presented in Fig. 20 and Table 5.

3.12. Survival analysis

Utilizing the UALCAN database and the pancreatic adenocarcinoma TCGA data (TCGA-PAAD), a survival analysis was conducted. In PPI and ceRNA networks, hub genes were used in a survival analysis. The difference had a log-rank P value below 0.05, indicating that it was statistically significant. Therefore, in patients with PDAC, HRAS, MDM2, PPARG, STAT1, UBE2L6, SNHG14, has-miR-21, has-miR-125a, and has-miR-212 showed a strong link with a shorter overall survival time (Fig. 21).

4. Discussion

PDAC is a highly heterogeneous tumor that is associated with high level of molecular complexity. Therefore, high throughput transcriptome analyses particularly at the level of single cell are needed to identify novel molecules involved in its onset and progression. Herein, we used an *in silico* approach for analysis of single cell RNA-seq data to identify differentially expressed genes and pathways between PDAC samples and adjacent non-tumoral samples. Our approach led to identification of 1462 DEmRNAs, including 1389 downregulated DEmRNAs (like PRSS1 and CLPS) and 73 upregulated DEmRNAs (like HSPA1A and

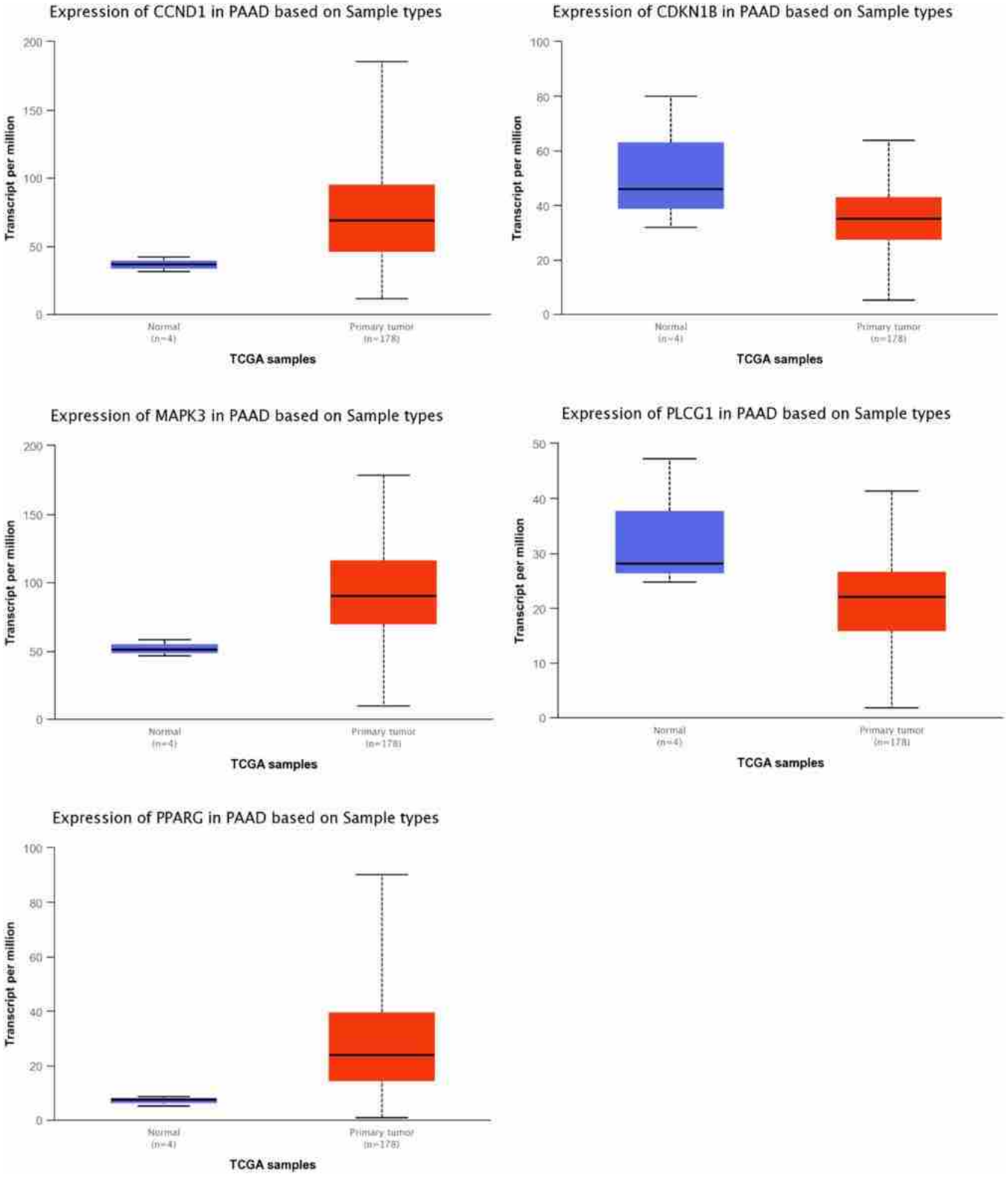

Fig. 20. based on the TCGA box plots showing the gene expression of hub genes in pancreatic adenocarcinoma and normal samples, hub gene expression is displayed in pancreatic cancer and normal samples respectively as red and blue boxes.

Table 5
Statistical significance of hub genes based on sample types in pancreatic adenocarcinoma TCGA data.

Hub genes	Statistical significance of expression value*
CCND1	1.09950004656412E-09
CDKN1B	4.917600E-02
MAPK3	5.91380000000141E-05
PLCG1	2.678400E-02
PPARG	1.62447832963153E-12

* Low number (<10) of normal samples considered

SOCS3), 27 DElncRNAs, including 26 downregulated DElncRNAs (like LINC00472 and SNHG7) and 1 upregulated DElncRNA (SNHG5). Previous studies have revealed presence of PRSS1 intron mutations in patients with pancreatic cancer as well as those with chronic pancreatitis [10]. In fact, mutations in this gene has been regarded as a possible mechanism for pancreatic carcinogenesis [19]. Contrary to our results, SOCS3 has been shown to negatively regulate JAK-STAT, thus its down-regulation has been found to be associated with the oncogenesis of pancreatic cancer [38]. Finally, SNHG5 is an oncogenic lncRNA that promotes proliferation, migration and metastasis of colorectal cancer cells [42].

Among related CCs, BPs and MFs have been those related to immune responses such as MHC protein complex and antigen processing and presentation. This finding is in line with the observed immunosuppressive microenvironment in PDAC, and attenuation of intratumoral activity of immune response in by inhibitory signals that suppress immune effector functions [5].

Moreover, we detected up-regulation of three pathways, including Protein processing in endoplasmic reticulum, Osteoclast differentiation, MAPK signaling pathway and Spliceosome in PDAC. Besides, SNHG14, OIP5-AS1, PHF1, LINC00324, SNHG7, hsa-miR-107, hsa-miR-125a-5p, hsa-miR-194, hsa-miR-18a, hsa-miR-21, hsa-miR-212, hsa-miR-27b, hsa-miR-27a, hsa-miR-31 and hsa-miR-34a have been found to be involved in the construction of ceRNA network in PDAC. These signaling pathways and constituents of ceRNA network are possible candidates for design of anti-cancer therapies.

Finally, HRAS, MDM2, PPARG, STAT1, UBE2L6, SNHG14, has-miR-21, has-miR-125a, and has-miR-212 have been demonstrated to be linked with a shorter overall survival time of patients with PDAC. Therefore, assessment of their expression can help in design of personalized strategies for management of PDAC.

In brief, in the current study, we listed a number of dysregulated signaling pathways, abnormally expressed genes and aberrant cellular functions in PDAC which can be used as possible biomarkers and therapeutic targets in this type of cancer.

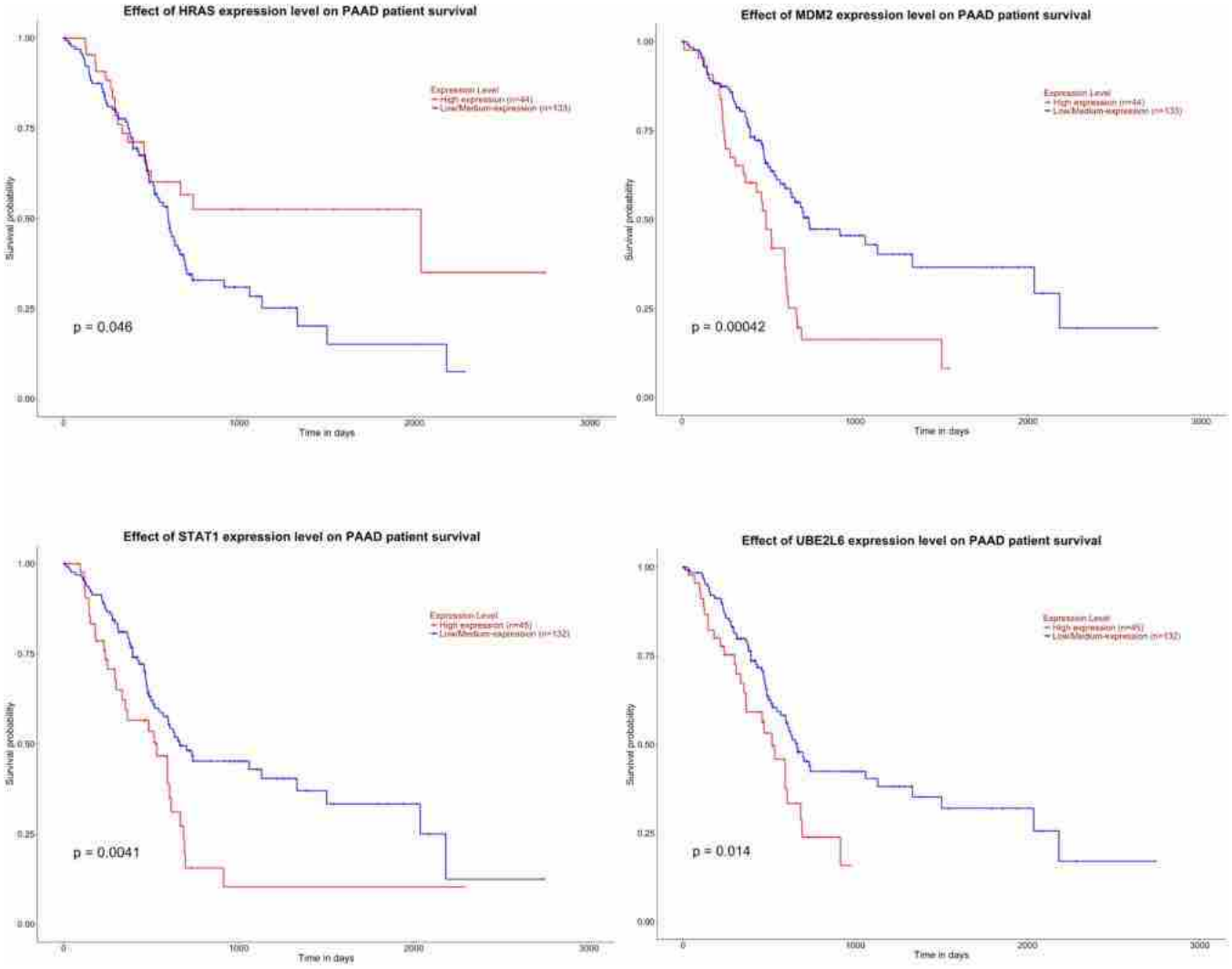

Fig. 21. The overall survival of pancreatic adenocarcinoma patients is related to the Kaplan-Meier survival curves of HRAS, MDM2, PPARG, STAT1, UBE2L6, SNHG14, has-miR-21, has-miR-125a and has-miR-212.

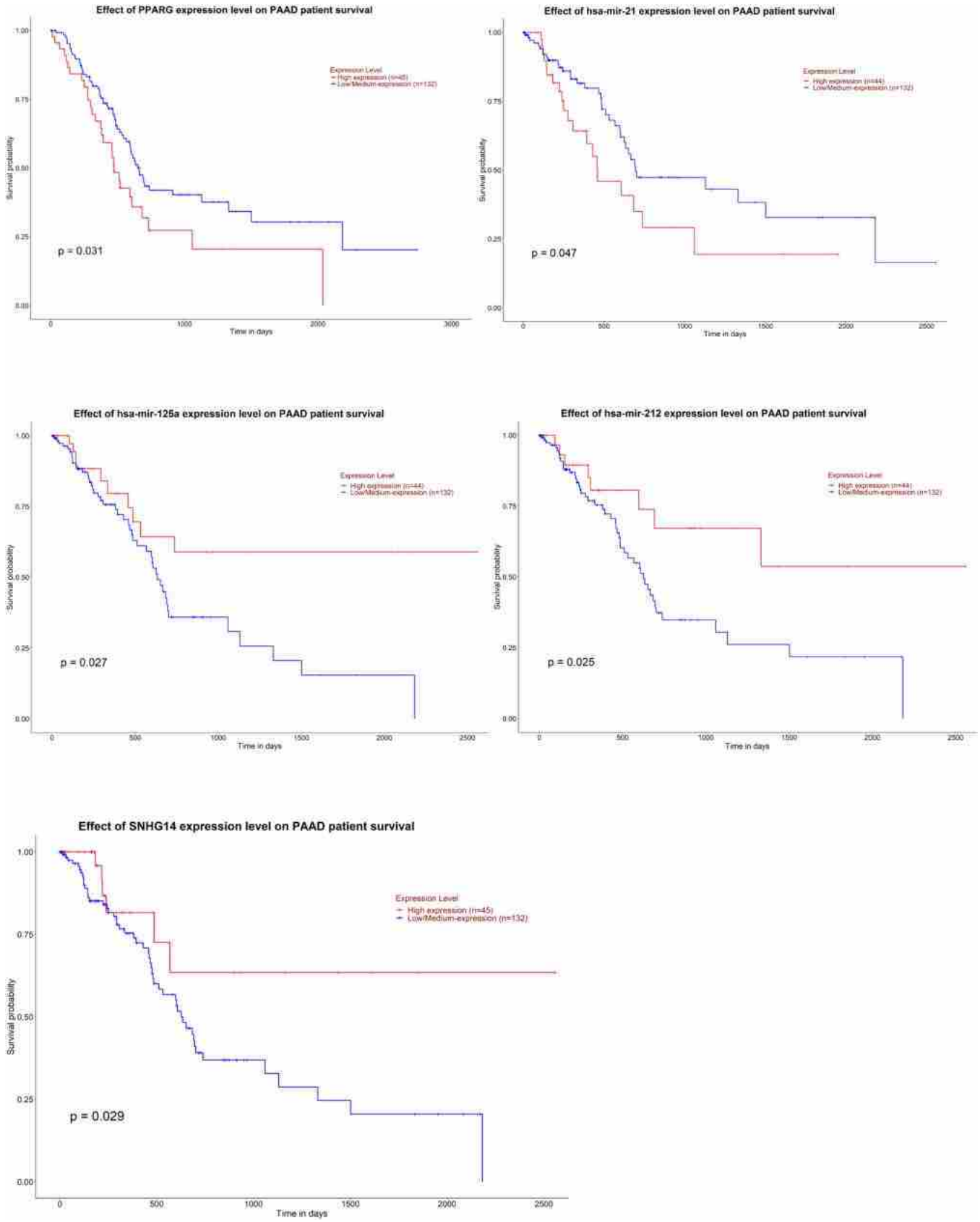

Fig. 21. (*continued*).

Ethics approval and consent to participant

Not applicable.

Funding

Not applicable.

CRediT authorship contribution statement

MT designed and supervised the study. **SGF and TL** wrote the draft and revised it. **AS, BMH and EJ** collected the data and designed the figures and tables. **AS and MT** performed the bioinformatic analysis. All the authors read the submitted version and approved it.

Declaration of Competing Interest

The authors declare they have no conflict of interest.

Acknowledgement

The authors would like to thank the Clinical Research Development Unit (CRDU) of Loghman Hakim Hospital, Shahid Beheshti University of Medical Sciences, Tehran, Iran for their support, cooperation and assistance throughout the period of study.

Consent of publication

Not applicable.

References

[1] V. Agarwal, G.W. Bell, J.W. Nam, D.P. Bartel, Predicting effective microRNA target sites in mammalian mRNAs, Elife 4 (2015).
[2] D. Aran, A.P. Looney, L. Liu, E. Wu, V. Fong, A. Hsu, S. Chak, R.P. Naikawadi, P. J. Wolters, A.R. Abate, A.J. Butte, M. Bhattacharya, Reference-based analysis of lung single-cell sequencing reveals a transitional profibrotic macrophage, Nat. Immunol. 20 (2019) 163–172.
[3] M. Bou Zerdan, M. Shatila, D. Sarwal, Y. Bouferraa, M. Bou Zerdan, S. Allam, M. Ramovic, S. Graziano, Single Cell RNA sequencing: a new frontier in pancreatic ductal adenocarcinoma, Cancers 14 (2022) 4589.
[4] D.S. Chandrashekar, B. Bashel, S.A.H. Balasubramanya, C.J. Creighton, I. Ponce-Rodriguez, B. Chakravarthi, S. Varambally, UALCAN: a portal for facilitating tumor subgroup gene expression and survival analyses, Neoplasia 19 (2017) 649–658.
[5] J.H. Chang, Y. Jiang, V.G. Pillarisetty, Role of immune cells in pancreatic cancer from bench to clinical application: An updated review, Medicine 95 (2016), e5541.
[6] Y. Chen, X. Wang, miRDB: an online database for prediction of functional microRNA targets, Nucleic Acids Res 48 (2020) D127–d131.
[7] C.-H. Chin, S.-H. Chen, H.-H. Wu, C.-W. Ho, M.-T. Ko, C.-Y. Lin, cytoHubba: identifying hub objects and sub-networks from complex interactome, BMC Syst. Biol. 8 (2014) S11.
[8] M. Enge, H.E. Arda, M. Mignardi, J. Beausang, R. Bottino, S.K. Kim, S.R. Quake, Single-Cell Analysis of Human Pancreas Reveals Transcriptional Signatures of Aging and Somatic Mutation Patterns. Cell 171 (2017) 321–330.e314.
[9] M. Fathi, S. Ghafouri-Fard, A. Abak, M. Taheri, Emerging roles of miRNAs in the development of pancreatic cancer, Biomed. Pharmacother. 141 (2021).
[10] F. Gao, Q.C. Liu, S. Zhang, Z.H. Zhuang, C.Z. Lin, X.H. Lin, PRSS1 intron mutations in patients with pancreatic cancer and chronic pancreatitis, Mol. Med. Rep. 5 (2012) 449–451.
[11] S. Ghafouri-Fard, M. Fathi, T. Zhai, M. Taheri, P. Dong, Lncrnas: novel biomarkers for pancreatic cancer, Biomolecules 11 (2021).
[12] R. Grützmann, H. Boriss, O. Ammerpohl, J. Lüttges, H. Kalthoff, H.K. Schackert, G. Klöppel, H.D. Saeger, C. Pilarsky, Meta-analysis of microarray data on pancreatic cancer defines a set of commonly dysregulated genes, Oncogene 24 (2005) 5079–5088.
[13] L.L. Guo, C.H. Song, P. Wang, L.P. Dai, J.Y. Zhang, K.J. Wang, Competing endogenous RNA networks and gastric cancer, World J. Gastroenterol. 21 (2015) 11680–11687.
[14] Y. Hao, S. Hao, E. Andersen-Nissen, W.M. Mauck, 3rd, S. Zheng, A. Butler, M.J. Lee, A.J. Wilk, C. Darby, M. Zager, P. Hoffman, M. Stoeckius, E. Papalexi, E.P. Mimitou, J. Jain, A. Srivastava, T. Stuart, L.M. Fleming, B. Yeung, A.J. Rogers, J.M. McElrath, C.A. Blish, R. Gottardo, P. Smibert, R. Satija, Integrated analysis of multimodal single-cell data. Cell 184 (2021) 3573–3587.e3529.
[15] H.Y. Huang, Y.C. Lin, J. Li, K.Y. Huang, S. Shrestha, H.C. Hong, Y. Tang, Y.G. Chen, C.N. Jin, Y. Yu, J.T. Xu, Y.M. Li, X.X. Cai, Z.Y. Zhou, X.H. Chen, Y.Y. Pei, L. Hu, J. J. Su, S.D. Cui, F. Wang, Y.Y. Xie, S.Y. Ding, M.F. Luo, C.H. Chou, N.W. Chang, K. W. Chen, Y.H. Cheng, X.H. Wan, W.L. Hsu, T.Y. Lee, F.X. Wei, H.D. Huang, miRTarBase 2020: updates to the experimentally validated microRNA-target interaction database, Nucleic Acids Res 48 (2020) D148–d154.
[16] J. Jia, H. Parikh, W. Xiao, J.W. Hoskins, H. Pflicke, X. Liu, I. Collins, W. Zhou, Z. Wang, J. Powell, An integrated transcriptome and epigenome analysis identifies a novel candidate gene for pancreatic cancer, BMC Med. Genom. 6 (2013) 1–13.
[17] M. Kanehisa, S. Goto, KEGG: kyoto encyclopedia of genes and genomes, Nucleic Acids Res 28 (2000) 27–30.
[18] J. Kleeff, M. Korc, M. Apte, C. La Vecchia, C.D. Johnson, A.V. Biankin, R.E. Neale, M. Tempero, D.A. Tuveson, R.H. Hruban, Pancreatic cancer, Nat. Rev. Dis. Prim. 2 (2016) 1–22.
[19] Q. Liu, L. Guo, S. Zhang, J. Wang, X. Lin, F. Gao, PRSS1 mutation: a possible pathomechanism of pancreatic carcinogenesis and pancreatic cancer, Mol. Med. 25 (2019) 1–11.
[20] Y. Liu, A. Beyer, R. Aebersold, On the dependency of cellular protein levels on mRNA abundance, Cell 165 (2016) 535–550.
[21] M.I. Love, W. Huber, S. Anders, Moderated estimation of fold change and dispersion for RNA-seq data with DESeq2, Genome Biol. 15 (2014) 1–21.
[22] W. Luo, C. Brouwer, Pathview: an R/Bioconductor package for pathway-based data integration and visualization, Bioinformatics 29 (2013) 1830–1831.
[23] W. Luo, M.S. Friedman, K. Shedden, K.D. Hankenson, P.J. Woolf, BMC Bioinformatics, 10, generally applicable gene set enrichment for pathway analysis, GAGE, 2009, p. 161.
[24] Y. Mao, J. Shen, Y. Lu, K. Lin, H. Wang, Y. Li, P. Chang, M.G. Walker, D. Li, RNA sequencing analyses reveal novel differentially expressed genes and pathways in pancreatic cancer, Oncotarget 8 (2017) 42537–42547.
[25] B.M. Paisley, Y. Liu, GeneMarkeR: a database and user interface for scRNA-seq marker genes, Front Genet 12 (2021), 763431.
[26] A.K. Ranjan, M.V. Joglekar, A.A. Hardikar, Endothelial cells in pancreatic islet development and function, Islets 1 (2009) 2–9.
[27] A. Sayad, S. Najafi, B.M. Hussen, E. Jamali, M. Taheri, S. Ghafouri-Fard, The role of circular RNAs in pancreatic cancer: new players in tumorigenesis and potential biomarkers, Pathol. Res. Pract. 232 (2022).
[28] N. Schaum , J. Karkanias , N.F. Neff , A.P. May , S.R. Quake , T. Wyss-Coray , S. Darmanis , J. Batson , O. Botvinnik , M.B. Chen , S. Chen , F. Green , R.C. Jones , A. Maynard , L. Penland , A.O. Pisco , R.V. Sit , G.M. Stanley , J.T. Webber , F. Zanini , A.S. Baghel , I. Bakerman , I. Bansal , D. Berdnik , B. Bilen , D. Brownfield , C. Cain , M.B. Chen , S. Chen , M. Cho , G. Cirolia , S.D. Conley , S. Darmanis , A. Demers , K. Demir , A. de Morree , T. Divita , H. du Bois , L.B.T. Dulgeroff , H. Ebadi , F.H. Espinoza , M. Fish , Q. Gan , B.M. George , A. Gillich , F. Green , G. Genetiano , X. Gu , G.S. Gulati , Y. Hang , S. Hosseinzadeh , A. Huang , T. Iram , T. Isobe , F. Ives , R.C. Jones , K.S. Kao , G. Karnam , A.M. Kershner , B.M. Kiss , W. Kong , M.E. Kumar , J.Y. Lam , D.P. Lee , S.E. Lee , G. Li , Q. Li , L. Liu , A. Lo , W.-J. Lu , A. Manjunath , A.P. May , K.L. May , O.L. May , A. Maynard , M. McKay , R.J. Metzger , M. Mignardi , D. Min , A.N. Nabhan , N.F. Neff , K.M. Ng , J. Noh , R. Patkar , W.C. Peng , L. Penland , R. Puccinelli , E.J. Rulifson , N. Schaum , S.S. Sikandar , R. Sinha , R.V. Sit , K. Szade , W. Tan , C. Tato , K. Tellez , K.J. Travaglini , C. Tropini , L. Waldburger , L.J. van Weele , M.N. Wosczyna , J. Xiang , S. Xue , J. Youngyunpipatkul , F. Zanini , M.E. Zardeneta , F. Zhang , L. Zhou , I. Bansal , S. Chen , M. Cho , G. Cirolia , S. Darmanis , A. Demers , T. Divita , H. Ebadi , G. Genetiano , F. Green , S. Hosseinzadeh , F. Ives , A. Lo , A.P. May , A. Maynard , M. McKay , N.F. Neff , L. Penland , R.V. Sit , W. Tan , L. Waldburger , J. Youngyunpipatkul , J. Batson , O. Botvinnik , P. Castro , D. Croote , S. Darmanis , J. L. DeRisi , J. Karkanias , A.O. Pisco , G.M. Stanley , J.T. Webber , F. Zanini , A.S. Baghel , I. Bakerman , J. Batson , B. Bilen , O. Botvinnik , D. Brownfield , M.B. Chen , S. Darmanis , K. Demir , A. de Morree , H. Ebadi , F.H. Espinoza , M. Fish , Q. Gan , B.M. George , A. Gillich , X. Gu , G.S. Gulati , Y. Hang , A. Huang , T. Iram , T. Isobe , G. Karnam , A.M. Kershner , B.M. Kiss , W. Kong , C.S. Kuo , J.Y. Lam , B. Lehallier , G. Li , Q. Li , L. Liu , W.-J. Lu , D. Min , A.N. Nabhan , K.M. Ng , P.K. Nguyen , R. Patkar , W.C. Peng , L. Penland , E.J. Rulifson , N. Schaum , S.S. Sikandar , R. Sinha , K. Szade , S.Y. Tan , K. Tellez , K.J. Travaglini , C. Tropini , L.J. van Weele , B.M. Wang , M.N. Wosczyna , J. Xiang , H. Yousef , L. Zhou , J. Batson , O. Botvinnik , S. Chen , S. Darmanis , F. Green , A.P. May , A. Maynard , A.O. Pisco , S.R. Quake , N. Schaum , G.M. Stanley , J.T. Webber , T. Wyss-Coray , F. Zanini , P.A. Beachy , C.K. F. Chan , A. de Morree , B.M. George , G.S. Gulati , Y. Hang , K.C. Huang , T. Iram , T. Isobe , A.M. Kershner , B.M. Kiss , W. Kong , G. Li , Q. Li , L. Liu , W.-J. Lu , A.N. Nabhan , K.M. Ng , P.K. Nguyen , W.C. Peng , E.J. Rulifson , N. Schaum , S.S. Sikandar , R. Sinha , K. Szade , K.J. Travaglini , C. Tropini , B.M. Wang , K. Weinberg , M.N. Wosczyna , S.M. Wu , H. Yousef , B.A. Barres , P.A. Beachy , C.K.F. Chan , M.F. Clarke , S. Darmanis , K.C. Huang , J. Karkanias , S.K. Kim , M.A. Krasnow , M.E. Kumar , C.S. Kuo , A.P. May , R.J. Metzger , N.F. Neff , R. Nusse , P. K. Nguyen , T.A. Rando , J. Sonnenburg , B.M. Wang , K. Weinberg , I.L. Weissman , S.M. Wu , S.R. Quake , T. Wyss-Coray , C. The Tabula Muris , c. Overall , c. Logistical , c. Organ, processing, p. Library, sequencing, a. Computational data, a. Cell type, g. Writing, g. Supplemental text writing, i. Principal, Single-cell transcriptomics of 20 mouse organs creates a Tabula Muris. Nature 562 (2018) 367–372.
[29] P. Shannon, A. Markiel, O. Ozier, N.S. Baliga, J.T. Wang, D. Ramage, N. Amin, B. Schwikowski, T. Ideker, Cytoscape: a software environment for integrated models of biomolecular interaction networks, Genome Res 13 (2003) 2498–2504.
[30] S. Sharbati-Tehrani, B. Kutz-Lohroff, R. Bergbauer, J. Scholven, R. Einspanier, miR-Q: a novel quantitative RT-PCR approach for the expression profiling of small RNA molecules such as miRNAs in a complex sample, BMC Mol. Biol. 9 (2008) 34.
[31] C. Sticht, C. De La Torre, A. Parveen, N. Gretz, miRWalk: An online resource for prediction of microRNA binding sites, PLoS One 13 (2018), e0206239.

[32] D. Szklarczyk, A. Franceschini, S. Wyder, K. Forslund, D. Heller, J. Huerta-Cepas, M. Simonovic, A. Roth, A. Santos, K.P. Tsafou, M. Kuhn, P. Bork, L.J. Jensen, C. von Mering, STRING v10: protein-protein interaction networks, integrated over the tree of life, Nucleic Acids Res 43 (2015) D447–452.
[33] S. Tweedie, B. Braschi, K. Gray, T.E.M. Jones, R.L. Seal, B. Yates, E.A. Bruford, Genenames.org: the HGNC and VGNC resources in 2021, Nucleic Acids Res 49 (2021) D939–d946.
[34] N. Waddell, M. Pajic, A.-M. Patch, D.K. Chang, K.S. Kassahn, P. Bailey, A.L. Johns, D. Miller, K. Nones, K. Quek, Whole genomes redefine the mutational landscape of pancreatic cancer, Nature 518 (2015) 495–501.
[35] Z. Wang, M. Gerstein, M. Snyder, RNA-Seq: a revolutionary tool for transcriptomics, Nat. Rev. Genet. 10 (2009) 57–63.
[36] T. Wu, E. Hu, S. Xu, M. Chen, P. Guo, Z. Dai, T. Feng, L. Zhou, W. Tang, L. Zhan, X. Fu, S. Liu, X. Bo, G. Yu, clusterProfiler 4.0: a universal enrichment tool for interpreting omics data, Innov. (Camb.) 2 (2021), 100141.
[37] B. Xie, Q. Ding, H. Han, D. Wu, miRCancer: a microRNA-cancer association database constructed by text mining on literature, Bioinformatics 29 (2013) 638–644.
[38] J. Xie, J.T. Wen, X.J. Xue, K.P. Zhang, X.Z. Wang, H.H. Cheng, MiR-221 inhibits proliferation of pancreatic cancer cells via down regulation of SOCS3, Eur. Rev. Med. Pharmacol. Sci. 22 (2018) 1914–1921.
[39] Y. Xu, J. Chen, Z. Yang, L. Xu, Identification of RNA expression profiles in thyroid cancer to construct a competing endogenous RNA (ceRNA) network of mRNAs, long noncoding RNAs (lncRNAs), and microRNAs (miRNAs), Med Sci. Monit. 25 (2019) 1140–1154.
[40] M. Yu, D.T. Ting, S.L. Stott, B.S. Wittner, F. Ozsolak, S. Paul, J.C. Ciciliano, M. E. Smas, D. Winokur, A.J. Gilman, RNA sequencing of pancreatic circulating tumour cells implicates WNT signalling in metastasis, Nature 487 (2012) 510–513.
[41] M.M. Zanone, E. Favaro, G. Camussi, From endothelial to beta cells: insights into pancreatic islet microendothelium, Curr. Diabetes Rev. 4 (2008) 1–9.
[42] M. Zhang, Y. Li, H. Wang, W. Yu, S. Lin, J. Guo, LncRNA SNHG5 affects cell proliferation, metastasis and migration of colorectal cancer through regulating miR-132-3p/CREB5, Cancer Biol. Ther. 20 (2019) 524–536.
[43] Z. Zhou, B. Sun, S. Huang, L. Zhao, Roles of circular RNAs in immune regulation and autoimmune diseases, Cell Death Dis. 10 (2019), 503-503.